Physics – Uspekhi **60** (7) 667 – 693 (2017)

REVIEWS OF TOPICAL PROBLEMS

PACS numbers: 12.38.Aw, 12.39.Ki, 12.39.Pn

Chiral symmetry and the properties of hadrons in the generalized Nambu – Jona-Lasinio model

Yu S Kalashnikova, A V Nefed'ev, J E F T Ribeiro

DOI: https://doi.org/10.3367/UFNe.2016.11.037966

Contents

Abstract. Various aspects of the generalized Nambu – Jona-Lasinio model of QCD in four dimensions are reviewed. The properties of mesonic excitations are discussed in detail, with special attention on the chiral pion. Spontaneous chiral symmetry breaking in a vacuum and effective chiral symmetry restoration in the spectrum of highly excited mesons and baryons are described microscopically.

Keywords: strong interactions, quantum chromodynamics, chiral symmetry, quark model, properties of hadrons, chiral pion

Yu S Kalashnikova National Research Center 'Kurchatov Institute', Alikhanov Institute of Theoretical and Experimental Physics, ul. B Cheremushkinskaya 25, 117218 Moscow, Russian Federation; National Research Nuclear University 'MEPhI', Kashirskoe shosse 31, 115409 Moscow, Russian Federation
A V Nefed'ev National Research Center 'Kurchatov Institute', Alikhanov Institute of Theoretical and Experimental Physics, ul. B Cheremushkinskaya 25, 117218 Moscow, Russian Federation; National Research Nuclear University 'MEPhI', Kashirskoe shosse 31, 115409 Moscow, Russian Federation; Moscow Institute of Physics and Technology (State University), Institutskii per. 9, 141700 Dolgoprudnyi, Moscow region, Russian Federation
E-mail: nefediev@itep.ru
J E F T Ribeiro Instituto Superior Técnico, Universidade de Lisboa, Av. Rovisco Pais 1, 1049-001 Lisboa, Portugal

Received 16 September 2016, revised 18 November 2016
Uspekhi Fizicheskikh Nauk **187** (7) 715 – 743 (2017)
DOI: https://doi.org/10.3367/UFNr.2016.11.037966
Translated by A V Nefed'ev; edited by A M Semikhatov

1. Introduction

Quark models of strong interactions have a long history, starting from the mid-20th century when the idea of hadrons composed of quarks was commonly accepted. And, as it happens, not only the number of various quark models but even the number of their types turned out to be quite large. For example, the so-called Coulomb + linear potential model in [1] describes heavy quarkonium spectra with rather good accuracy, which is clearly due to the heavy quark mass being much larger than the scale of strong interaction Λ_{QCD}. A naive kinematical relativization [2] of the quark model allows considering mesons made of light quarks, although the justification for the potential model approach is less obvious in this case. The given approach, as well as similar models, is simple, for numerical calculations as well; however, its range of applicability is very limited, and many phenomena inherent in quantum chromodynamics (QCD), which are of interest for the phenomenology of strong interactions, cannot be addressed in such a framework. Among them, the effect of spontaneous breaking of chiral symmetry in the QCD vacuum, its implications for the spectrum of hadrons, and the effective restoration of chiral symmetry in excited hadrons should be mentioned.

It is well known that in the chiral limit, the $\mathrm{SU(2)_L \times SU(2)_R}$ symmetry of the QCD Lagrangian is broken, and this affects the observed spectrum of hadrons. Thus, the spontaneous symmetry breaking $\mathrm{SU(2)_L \times SU(2)_R \to SU(2)}$ [3] manifests itself through the absence of low-lying hadrons populating multiplets of the $\mathrm{SU(2)_L \times SU(2)_R}$ group, through the Goldstone nature of the pion, in particular, through its vanishing mass (which is finite beyond the strict chiral limit, but quite small compared to the typical hadronic scale), through the nonzero value of the chiral condensate in the vacuum, and so on. Thus, chiral symmetry is realized nonlinearly in low-lying hadrons.

Meanwhile, there are good reasons to believe that the aforementioned symmetry is effectively restored in the spectrum of both excited baryons [4–6] and excited mesons [7–9]. A nice and convincing justification of such a restoration in the spectrum of excited hadrons was suggested in a recent paper [10], where the masses of light hadrons were extracted from the lattice configuration after the near-zero modes of the Dirac operator, responsible for the spontaneous chiral symmetry breaking [11], were artificially removed. The resulting mass spectrum demonstrated a remarkably high degeneracy pattern, including formation of chiral multiplets [12].

The full solution of QCD would yield a microscopic description of the effect of the spontaneous breaking of chiral symmetry. In the absence of such a solution, various approaches have been suggested aimed at identification of gluonic field configurations that could be responsible for chiral symmetry breaking. It is quite natural to relate chiral symmetry breaking to confinement, yet another prominent feature of QCD. For example, in the approach in [13], the confining kernel derived in the vacuum correlator method [14] gives rise to the interaction of light quarks with Nambu–Goldstone fields, thus yielding an effective chiral Lagrangian. The subject of the present review is a phenomenological approach that employs a simple ansatz for the confining kernel pertinent to the matter at hand. The approach gains experience from the 't Hooft model [15] of two-dimensional QCD in the limit of a large number of colors ($N_c \to \infty$).

First, we note that a microscopic description of the effect of spontaneous chiral symmetry breaking requires an intrinsically field theoretic approach that takes both particles and antiparticles into account on equal footing within the same formalism. And this necessity lies outside the scope of constituent quark models because they merely provide an essentially quantum mechanical approach, even if one considers relativistic kinematics. Formally, the problem stems from the fact that when working in the formalism of relativistic quantum-mechanical Hamiltonians, one is stuck with a particular (positive) sign of the energy while the contributions from the other (negative) sign of the energy are ignored. Such 'negative' solutions correspond to antiparticles, and hence the interplay of both positive and negative solutions leads to a Z-like (Zitterbewegung) trajectory of the particle, that is, to so-called Z-graphs. The problem can be traced to the spectrum: the Salpeter equation that emerges for the bound states is defined with the help of a single-component Hamiltonian that describes the particle, and therefore the resulting bound-state equation is derived without the Hamiltonian components related to antiparticles. Such an approximation is well justified for heavy particles; however, it is obviously misleading for light quarks and hence for the light hadrons built thereof, for the chiral pion in the first place.

The proper mechanism to account for the Zitterbewegung motion of particles can be established in terms of a matrix Hamiltonian and a two-component wave function. In [16], such an approach to the two-dimensional 't Hooft model was suggested and described in detail. The key approximations that allowed controlling the pair creation process are the limit of the large number of colors $N_c \to \infty$ (an introduction to this limit in QCD and related issues can be found in [17]). In addition, we note that the limit of the large number of degrees of freedom allows overriding [18] the Coleman no-go theorem, which forbids spontaneous breaking of chiral symmetry in two dimensions [19]. Additional simplifications in the model arise from the instantaneous type of interaction mediated by the two-dimensional gluon. To establish this last property, it is sufficient to count the number of the degrees of freedom for the two-dimensional gluon and then to arrive straightforwardly at the absence of the gluon transverse propagating degrees of freedom. The 't Hooft model in the axial gauge considered in [16] describes the interaction of two quark currents taken at equal time and mediated by the confining potential that depends on the one-dimensional interquark separation. The terms containing higher powers of the quark currents do not appear in this Hamiltonian, which is a reflection of the fact that all correlators of several gluonic fields either vanish or reduce to the powers of the bilocal correlator, which is merely the gluon propagator. As a result, there is only one irreducible field correlator $\langle\langle A_1 A_2\rangle\rangle = \langle A_1 A_2\rangle - \langle A_1\rangle\langle A_2\rangle = \langle A_1 A_2\rangle$, with all such irreducible correlators of higher orders vanishing. This result is exact in two dimensions and does not rely on any approximations or assumptions. A review of the 't Hooft model in the axial gauge can be found in [20].

In contrast to the two-dimensional case, the instantaneous nature of the interquark interaction and the absence in the Hamiltonian of terms with the product of more than two quark currents are approximations that allow building a realistic quark model, which we review in what follows. Thus, a quark model with quark currents endowed with an instantaneous interaction was suggested as a model for QCD about 30 years ago in [21–24] and was studied in detail in the Hamiltonian formalism in [25–30], as well as in later studies [31–35]. As was mentioned above, this model can be regarded as the four-dimensional generalization of the 't Hooft model in two dimensions. At the same time, the same model can also be viewed as the generalization of the four-dimensional Nambu–Jona-Lasinio (NJL) model [3] to a nonlocal interaction of the quark currents. It is important to note that in spite of its long history, the NJL model [3] still remains a useful and convenient tool for various studies in the physics of strong interactions. An important role in this was played by a detailed study of the connection between the model and QCD (see, e.g., [36, 37]) and by its further development (see reviews [38, 39]), which allow considerably extending the range of the problems where this model can be successfully used. An important feature of a Nambu–Jona-Lasinio-type model, hereinafter referred to as the generalized Nambu–Jona-Lasinio (GNJL) model, is the presence of a confining interaction, which allows using this model to address the problem of bound states and which also brings an intrinsic scale into the model.

The model is defined in terms of the Hamiltonian (for simplicity, only one quark flavor is considered, the generalization to the multi-flavor case being trivial)

$$\hat{H} = \int d^3x \bar{\psi}(\mathbf{x}, t)(-i\boldsymbol{\gamma} + m)\,\psi(\mathbf{x}, t)$$

$$+ \frac{1}{2}\int d^3x\, d^3y\, J^a_\mu(\mathbf{x}, t)\, K^{ab}_{\mu\nu}(\mathbf{x}-\mathbf{y})\, J^b_\nu(\mathbf{y}, t)\,, \tag{1}$$

where, as was explained above, the coupling of quark currents $J^a_\mu(\mathbf{x}, t) = \bar{\psi}_\alpha(\mathbf{x}, t)\,\gamma_\mu(\lambda^a/2)^\alpha_\beta\psi_\beta(\mathbf{x}, t)$ is parameterized with the help of the instantaneous kernel

$$K^{ab}_{\mu\nu}(\mathbf{x}-\mathbf{y}) = g_{\mu 0} g_{\nu 0} \delta_{ab} V_0\big(|\mathbf{x}-\mathbf{y}|\big) . \tag{2}$$

Hereinafter, the following notation is used:

- lower-case letters from the beginning of the Greek (Latin) alphabet, that is, α, β, and so on (a, b, and so on) are used for the color indices in the fundamental (adjoint) representation and range $1, 2, \ldots, N_c$ $(1, 2, \ldots, N_c^2 - 1)$;
- lower-case letters from the middle of the Greek alphabet (μ, ν, and so on) are used for those Lorentz indices that take values from 0 to 3;
- $\psi(\mathbf{x}, t)$ is the fermion (quark) field; $\bar{\psi} = \psi^\dagger \gamma_0$;
- m is the mass of the quark (the chiral limit implies that $m = 0$);
- $\gamma^\mu = (\gamma_0, \boldsymbol{\gamma})$ are the Dirac matrices;
- λ are the color matrices (generators of the $SU(N_c)$ group);
- $g_{\mu\nu}$ is the Minkowski metric tensor; and
- δ_{ab} is the Kronecker symbol.

Typically, the confining potential is chosen in a power-law form,

$$V_0\big(|\mathbf{x}|\big) = K_0^{\alpha+1} |\mathbf{x}|^\alpha , \quad 0 \leqslant \alpha \leqslant 2 , \tag{3}$$

where K_0 is the parameter of the model, with the dimension of mass. The qualitative predictions of the model are independent of the particular form of the potential if it only is confining for colored objects, on the one hand, and demonstrates moderate growth with the interquark separation to avoid divergent integrals, on the other.

Boundary cases with $\alpha = 0$ and $\alpha = 2$ require special treatment. In particular, in the limit $\alpha \to 0$, the potential has to be redefined as

$$V_0\big(|\mathbf{x}|\big) \to \tilde{V}_0\big(|\mathbf{x}|\big) = K_0 \left. \frac{\big(K_0|\mathbf{x}|\big)^\alpha - 1}{\alpha} \right|_{\alpha \to 0} = K_0 \ln\big(K_0|\mathbf{x}|\big) , \tag{4}$$

and hence the resulting interaction is logarithmic. Strictly speaking, the potential can also be defined for negative values $\alpha > -1$ (for $\alpha = -1$, that is, for the Coulomb potential, the integrals become divergent again; see [32] for details). However, negative powers of α do not provide confinement for quarks, and they are disregarded in what follows.

In the limit $\alpha = 2$, the Fourier transform of the potential reduces to the Laplacian of the three-dimensional δ-function, and therefore, by taking integrals by parts, we can turn all integral equations into second-order differential equations, which are much simpler to deal with from the technical standpoint. This explains why such a choice is quite popular in the literature (see, e.g., [21–29]). Still larger values of α, $\alpha > 2$, lead to divergent integrals and are not considered (a detailed discussion of the problem can be found in [21–23, 32]). More realistic quantitative predictions can be made with the help of the linear confinement [40–44].

As was mentioned above, qualitative results are insensitive to the particular form of the potential, and therefore it is not fixed in most cases in what follows. If, however, a quantitative investigation of equations is needed, the potential is chosen in the most appropriate power-law form, as in Eqn (3).

The GNJL model meets a wide set of requirements, such as (a) the ability to account for relativistic effects; (b) the presence of an explicit confining force (and therefore it can be employed to address various questions related to bound states of quarks, including excited hadrons); (c) chiral symmetry (for $m = 0$); and (d) the ability to describe the effect of spontaneous chiral symmetry breaking in a vacuum. The last point deserves an additional remark. In particular, the model satisfies all low-energy theorems such as the Gell-Mann–Oakes-Renner relation [45] (see [21–23]), the Goldberger–Treiman relation [46] (see [47]), the Adler self-consistency condition [48], and the Weinberg theorem [49] (see [50]). At the same time, the model has an attractive feature to microscopically describe the phenomenon of spontaneous breaking of chiral symmetry in a vacuum and its effective restoration in the spectrum of excited hadrons. These questions are discussed in detail in this review. Furthermore, because the effects of chiral symmetry breaking and restoration are closely related to the problem of the Lorentz nature of the confining interaction in quarkonia, that issue is also addressed in this review.

2. Bardeen–Cooper–Schrieffer approximation, mass-gap equation, and chirally broken vacuum

A convenient approach to studies of the model described by Hamiltonian (1) is the Bogoliubov–Valatin transformation, which allows proceeding from 'bare' quarks, which are the relevant degrees of freedom in a chirally symmetric vacuum, to 'dressed' quarks, which are the physical degrees of freedom in the chirally broken vacuum [25–29]. The quark field $\psi_\alpha(\mathbf{x}, t)$ is defined in terms of annihilation and creation operators $\hat{b}$, $\hat{d}$ and $\hat{b}^\dagger$, $\hat{d}^\dagger$, and takes the form

$$\psi_\alpha(\mathbf{x}, t) = \sum_{s=\uparrow,\downarrow} \int \frac{\mathrm{d}^3 p}{(2\pi)^3} \exp(\mathrm{i}\mathbf{p}\mathbf{x}) \times \big[\hat{b}_{\alpha s}(\mathbf{p}, t)\, u_s(\mathbf{p}) + \hat{d}^\dagger_{\alpha s}(-\mathbf{p}, t)\, v_{-s}(-\mathbf{p})\big] , \tag{5}$$

$$u_s(\mathbf{p}) = \frac{1}{\sqrt{2}} \left[\sqrt{1 + \sin\varphi_p} + \sqrt{1 - \sin\varphi_p}\, \boldsymbol{\alpha}\hat{\mathbf{p}}\right] u_s(0) ,$$
$$v_{-s}(-\mathbf{p}) = \frac{1}{\sqrt{2}} \left[\sqrt{1 + \sin\varphi_p} - \sqrt{1 - \sin\varphi_p}\, \boldsymbol{\alpha}\hat{\mathbf{p}}\right] v_{-s}(0) , \tag{6}$$

$$\hat{b}_s(\mathbf{p}, t) = \exp(\mathrm{i}E_p t)\, \hat{b}_s(\mathbf{p}, 0) ,$$
$$\hat{d}_s(-\mathbf{p}, t) = \exp(\mathrm{i}E_p t)\, \hat{d}_s(-\mathbf{p}, 0) . \tag{7}$$

Here, the rest-frame bispinors are defined as

$$u_s(0) = \begin{pmatrix} w_s \\ 0 \end{pmatrix} , \quad v_{-s}(0) = -\mathrm{i}\gamma_2 u_s^*(0) = \begin{pmatrix} 0 \\ \mathrm{i}\sigma_2 w_s^* \end{pmatrix} , \tag{8}$$

where γ_2 (σ_2) is the second Dirac (Pauli) matrix, $s = \pm 1$ labels the spin eigenstates, whence $(w_s)_i = \delta_{si}$, and E_p is the dressed-quark energy. The quantity φ_p, which parameterizes the Bogoliubov–Valatin transformation, is known as the chiral angle and is defined with the boundary conditions $\varphi_p(p = 0) = \pi/2$ and $\varphi_p(p \to \infty) = 0$.

After normal ordering [1] in terms of the dressed creation and annihilation operators, Hamiltonian (1) takes the

[1] In this review, normal ordering of operators is indicated by colons, for example, $:\hat{H}_2:$.

form

$$\hat{H} = E_{\text{vac}} + :\hat{H}_2: + :\hat{H}_4:, \tag{9}$$

$$E_{\text{vac}}[\varphi_p] = -\frac{1}{2}\, gV \int \frac{d^3p}{(2\pi)^3}\,(A_p \sin\varphi_p + B_p \cos\varphi_p)\,, \tag{10}$$

where V is the three-dimensional volume and the factor g counts the total number of degrees of freedom for each quark, $g = (2S+1)\,N_c$, where $2S+1$ (with $S = 1/2$) is the number of quark spin projections (in the multi-flavor case, g is to be additionally multiplied by the number of flavors N_f). The functions of the momentum A_p and B_p are given by the formulas

$$\begin{aligned} A_p &= m + \frac{1}{2}\int \frac{d^3k}{(2\pi)^3}\, V(\mathbf{p}-\mathbf{k})\, \sin\varphi_k\,, \\ B_p &= p + \frac{1}{2}\int \frac{d^3k}{(2\pi)^3}\, \hat{\mathbf{p}}\hat{\mathbf{k}}\, V(\mathbf{p}-\mathbf{k})\, \cos\varphi_k\,, \end{aligned} \tag{11}$$

where the hats in $\hat{\mathbf{p}}$ and $\hat{\mathbf{k}}$ denote unit vectors for the respective momenta (hats over scalar quantities identify operators: see, e.g., (5)), $V = C_F V_0$, and $C_F = N_c^2 - 1)/(2N_c)$ is the eigenvalue of the fundamental Casimir operator. To ensure that the potential takes finite values in the limit $N_c \to \infty$, its strength is subject to an appropriate rescaling, that is, $K_0^{\alpha+1} N_c \underset{N_c\to\infty}{\longrightarrow} \text{const}$.

The explicit form of the chiral angle φ_p is determined from the requirement that the vacuum energy be kept at the minimum. For a qualitative investigation of the properties of the corresponding functional (10), it is convenient to use the following trick [30]. We suppose that the given functional has a minimum at a particular function $\varphi_0(p)$. Then, if evaluated at a rescaled function $\varphi_0(p/\xi)$, with $0 \leqslant \xi < \infty$, it must take larger values for all $\xi \neq 1$, and it should reproduce the above minimum at $\xi = 1$. Finally, taking the limit $\xi \to 0$ is equivalent to taking an infinitely large argument of the chiral angle, and because $\varphi_p(p \to \infty) \to 0$, such a limit is equivalent to the evaluation of the energy functional for the trivial, chirally symmetric solution. Thus, it proves instructive to study the behavior of the function $E_{\text{vac}}(\xi)$, which should have a minimum at $\xi = 1$. For simplicity, we consider the chiral limit and set $m = 0$. In this case, the only remaining dimensional parameter is the potential strength K_0. Then, by a redefinition of the integration variable in the functions A_p and B_p, $p \to p/\xi$, we readily arrive at

$$E_{\text{vac}}(\xi) = C_1 \xi^{d+1} + C_2 K_0^{\alpha+1} \xi^{d-\alpha}\,, \tag{12}$$

where D is the space–time dimension, $d = D - 1$, and C_1 and C_2 are two ξ-independent constants. For convenience, we measure the energy from the chirally symmetric solution $\varphi_p \equiv 0$, which corresponds to $\xi = 0$, that is, we set $E_{\text{vac}}(0) = 0$. Whether a minimum exists with a negative energy at $\xi = 1$ depends on the relation between the coefficients and the powers of the two contributions in expression (12). An interesting case is given by the limit $\alpha = d$. The 't Hooft model of two-dimensional QCD constitutes an example of such a limit for which $\alpha = d = 1$. Naively, one could expect that the second term in (12) turns into a constant in this limit and hence no nontrivial minimum can exist. However, this is not the case. It is important to note that for $\alpha = d$, the momentum integrals are logarithmically divergent in the infrared domain and, as such, they need a regulator, hereinafter denoted as λ. Then, in the given limit, the second term in formula (12) contains a logarithmic dependence on ξ,

$$E_{\text{vac}}^{(\alpha=d)}(\xi) = C_1 \xi^{d+1} + C_2 K_0^{d+1} \ln\left(\xi\, \frac{K_0}{\lambda}\right), \tag{13}$$

which entails two consequences: (i) a nontrivial minimum is possible if the coefficients C_1 and C_2 have different signs and (ii) the vacuum energy grows in approaching the trivial solution at $\xi = 0$. In other words, the chirally symmetric phase of the theory ceases to exist [30]. A similar conclusion for the 't Hooft model is made in [51].

For the GNJL model, $d = 3$, and in view of the restrictions on the value of the exponent α [see (3)], we always have $\alpha < d$. For a particular choice of the signs of the coefficients C_1 and C_2 in (12), this ensures the existence of a nontrivial solution that is energetically favorable compared to the trivial vacuum. By a straightforward check, we can ensure that, indeed, the needed signs are in evidence.

We note that the requirement that the vacuum energy be minimum guarantees at the same time that the quadratic part of the Hamiltonian, $:\hat{H}_2:$, is diagonal (that is, the anomalous terms of the form $\hat{b}^\dagger \hat{d}^\dagger - \hat{d}\hat{b}$ are absent), and the corresponding equation is known as the mass-gap equation [21–29],

$$A_p \cos\varphi_p = B_p \sin\varphi_p\,. \tag{14}$$

Then the dressed-quark dispersive law is

$$E_p = A_p \sin\varphi_p + B_p \cos\varphi_p\,. \tag{15}$$

It is easy to verify that the solution of the mass-gap equation for a free particle takes the form $\varphi_p = \arctan(m/p)$, and then the free dispersive law $E_p = \sqrt{p^2 + m^2}$ is readily reproduced. It is also worth mentioning that the same angle defines the Foldy–Wouthuysen transformation that brings the free Dirac Hamiltonian $H = \boldsymbol{\alpha}\mathbf{p} + \beta m$ to the diagonal form $H' = \beta E_p$. Such a deep connection between the chiral angle and the Foldy–Wouthuysen transformation persists for the nontrivial confining interaction and for the chiral angle given by the solution of the corresponding mass-gap equation (see, e.g., [20, 33]).

For an arbitrary power-law confining potential (3), the mass-gap equation takes the form (in the chiral limit, that is, for $m = 0$)

$$p^3 \sin\varphi_p = \frac{1}{2} K_0^3 \left(p^2 \varphi_p'' + 2p\varphi_p' + \sin 2\varphi_p\right) \tag{16}$$

for $\alpha = 2$ [21–29], and

$$\begin{aligned} p^3 \sin\varphi_p = K_0^{\alpha+1} \Gamma(\alpha+1)\, \sin\frac{\pi\alpha}{2} \int_{-\infty}^{\infty} \frac{dk}{2\pi} \\ \times \left[\frac{pk \sin(\varphi_k - \varphi_p)}{|p-k|^{\alpha+1}} + \frac{\cos\varphi_k \sin\varphi_p}{(\alpha-1)\,|p-k|^{\alpha-1}}\right] \end{aligned} \tag{17}$$

for $0 \leqslant \alpha < 2$ [32], where $\Gamma(\alpha+1)$ is the Euler gamma function. For convenience and to make the formulas more compact, the absolute value of the momentum p is formally extended to the domain $p < 0$ according to the rule $\cos\varphi_{-p} = -\cos\varphi_p$, $\sin\varphi_{-p} = \sin\varphi_p$. As was mentioned above, the mass-gap equation for the harmonic oscillator potential reduces to a second-order differential equation.

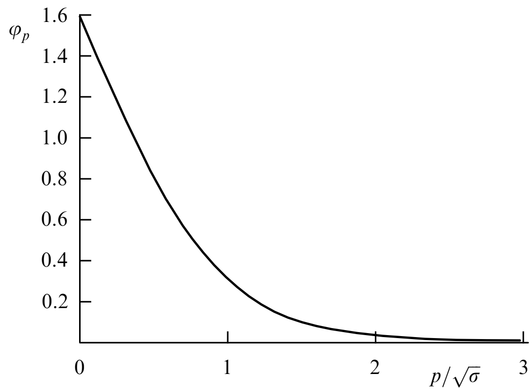

Figure 1. Solution of mass-gap equation (14) for $m = 0$ and for the linear confining potential $V(r) = \sigma r$, where the parameter σ has the dimension of mass squared.

In Fig. 1, the behavior of the chiral angle as a function of the momentum is exemplified by the solution of the mass-gap equation with a linear potential. Qualitatively, the shape of the curve does not depend on the particular form of the interquark potential. Further details of the formalism of the chiral angle can be found in [21–30, 33], whereas the details of various studies of the mass-gap equation can be found in [32] (for the four-dimensional theory) and in [16, 52] (for the two-dimensional theory). In particular, in some of the studies mentioned above, it was pointed out that the mass-gap equation supports the existence of 'excited' solutions, with the chiral angle possessing knots. Attempts to assign a physical meaning to such solutions can be found in [30, 31, 35]. In what follows, the problem of excited solutions (replicas) is not discussed, and we always understand the chiral angle of the form depicted in Fig. 1 as the nontrivial solution of the mass-gap equation.

For the chiral angle that is the solution of mass-gap equation (14), Hamiltonian (9) takes a diagonal form [25–29],

$$\hat{H} = E_{\text{vac}} + \sum_{\alpha=1}^{N_c} \sum_{s=\uparrow,\downarrow} \int \frac{\mathrm{d}^3 p}{(2\pi)^3}\, E_p \times \left[\hat{b}^\dagger_{\alpha s}(\mathbf{p})\, \hat{b}_{\alpha s}(\mathbf{p}) + \hat{d}^\dagger_{\alpha s}(-\mathbf{p})\, \hat{d}_{\alpha s}(-\mathbf{p})\right], \tag{18}$$

and the contribution of the omitted term $:\hat{H}_4:$ is suppressed as $1/\sqrt{N_c}$ in the large-N_c limit. In the literature, such an approximation is often referred to as the Bardeen–Cooper–Schrieffer (BCS) approximation, analogous to the similar approach by Bardeen, Cooper, and Schrieffer to the theory of superconductivity. The new, dressed operators b and d annihilate the vacuum $|0\rangle$ that is related to the trivial vacuum $|0\rangle_0$ annihilated by the bare operators, by the relations [25–29]

$$|0\rangle = \exp\left(Q - Q^\dagger\right)|0\rangle_0\,, \quad Q^\dagger = \frac{1}{2}\sum_{\mathbf{p}} \varphi_p C^\dagger_p\,,$$
$$C^\dagger_p = \sum_{\alpha=1}^{N_c} \sum_{s,s'=\uparrow,\downarrow} b^\dagger_{\alpha s}(\mathbf{p}) \left[(\boldsymbol{\sigma}\hat{\mathbf{p}})\,\mathrm{i}\sigma_2\right]_{ss'} d^\dagger_{\alpha s'}(\mathbf{p})\,, \tag{19}$$

where $\boldsymbol{\sigma}$ is given by the standard Pauli matrices and the operator $C^\dagger_p$ creates quark–antiquark pairs with the quantum numbers of the vacuum, $J^{PC} = 0^{++}$, that is, $^3P_0$ pairs. With the help of the (anti)commutation relations between the quark and antiquark operators, we can arrive at the following representation for the chirally broken (BCS) vacuum [25–29]:

$$|0\rangle = \prod_p \left(\sqrt{w_{0p}} + \frac{1}{\sqrt{2}}\sqrt{w_{1p}}\, C^\dagger_p + \frac{1}{2}\sqrt{w_{2p}}\, C^{\dagger 2}_p\right)|0\rangle_0\,, \tag{20}$$

where the coefficients take the form

$$w_{0p} = \cos^4\frac{\varphi_p}{2}\,, \quad w_{1p} = 2\sin^2\frac{\varphi_p}{2}\cos^2\frac{\varphi_p}{2}\,, \quad w_{2p} = \sin^4\frac{\varphi_p}{2} \tag{21}$$

and obey the condition $w_{0p} + w_{1p} + w_{2p} = 1$. We note that coefficients (21) support a natural interpretation in terms of the probabilities of finding one (w_{1p}) or two (w_{2p}) quark–antiquark pairs with the given relative momentum $2p$ in the new vacuum, or of finding no such pairs at all (w_{0p}) [34]. The Fermi statistics for the quarks and antiquarks makes it impossible to create more pairs with the same relative momentum.

It is straightforward to ensure, with the help of Eqns (20) and (21), that the wave function of the BCS vacuum is normalized (the trivial vacuum is assumed to be normalized as well),

$$\langle 0|0\rangle = \prod_p (w_{0p} + w_{1p} + w_{2p}) = 1\,, \tag{22}$$

and that the two vacua are orthogonal in the limit of an infinite volume V,

$$\langle 0|0\rangle_0 = \exp\left[\sum_p \ln\left(\cos^2\frac{\varphi_p}{2}\right)\right] = \exp\left[V\int\frac{\mathrm{d}^3 p}{(2\pi)^3}\ln\left(\cos^2\frac{\varphi_p}{2}\right)\right] \underset{V\to\infty}{\longrightarrow} 0\,. \tag{23}$$

It is easy to see that the BCS vacuum describes a cloud of strongly correlated quark–antiquark pairs at each point of the configuration space; the pair is created by the operator $\exp(Q - Q^\dagger)$, and this fact ensures the appearance of a nonzero quark–antiquark condensate in the vacuum,

$$\langle\bar{\psi}\psi\rangle = -\frac{N_c}{\pi^2}\int_0^\infty \mathrm{d}p\, p^2 \sin\varphi_p\,, \tag{24}$$

which vanishes at the trivial solution $\varphi_p \equiv 0$ but takes nonzero values for the nontrivial solution depicted in Fig. 1. Therefore, spontaneous chiral symmetry breaking occurs: the Hamiltonian of the theory is chirally symmetric, while the BCS vacuum is not. The large-momentum asymptotic form of the chiral angle is related to the chiral condensate as

$$\varphi_{p|m=0} \underset{p\to\infty}{\approx} -\frac{\pi}{N_c}\,\Gamma(\alpha+2)\, K_0^{\alpha+1}\sin\left(\frac{\pi\alpha}{2}\right)\frac{\langle\bar{\psi}\psi\rangle}{p^{\alpha+4}}\,. \tag{25}$$

It is instructive to note that, by the substitution $\varphi(p) \to \varphi(p/\xi)$ and a subsequent variable change $p = \xi p'$ in formula (24), it is easy to demonstrate that the chiral condensate scales as ξ^3. We can then rewrite (12) in the form of the function $E_{\text{vac}}(\langle\bar{\psi}\psi\rangle)$, which therefore supports the interpretation as an effective potential that reaches the minimum at a nonzero value of the chiral condensate.

An alternative approach to the derivation of the mass-gap equation is related to the Dyson equation for the dressed quark propagator, shown graphically in Fig. 2. Schematically, this equation can be represented as a sum of an infinite

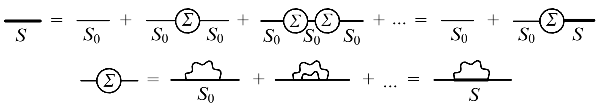

Figure 2. Graphical representation of the equation for the propagator and for the mass operator of the dressed quark.

series of loops,

$$S = S_0 + S_0 \Sigma S_0 + S_0 \Sigma S_0 \Sigma S_0 + \ldots = S_0 + S_0 \Sigma S\,, \tag{26}$$

with the mass operator given by the integral of the dressed propagator,

$$\begin{aligned} \mathrm{i}\Sigma(\mathbf{p}) &= \int \frac{\mathrm{d}^4 k}{(2\pi)^4}\, V(\mathbf{p}-\mathbf{k})\,\gamma_0 S(k_0, \mathbf{k})\,\gamma_0\,, \\ V(\mathbf{p}) &= C_{\mathrm{F}} V_0(\mathbf{p})\,, \quad C_{\mathrm{F}} = \frac{N_{\mathrm{c}}^2 - 1}{2N_{\mathrm{c}}}\,. \end{aligned} \tag{27}$$

The propagator $S(p_0, \mathbf{p})$ can be written with the help of projectors on the positive- and negative-energy solutions of the Dirac equation,

$$S(p_0, \mathbf{p}) = \frac{\Lambda^+(\mathbf{p})\,\gamma_0}{p_0 - E_p + \mathrm{i}0} + \frac{\Lambda^-(\mathbf{p})\,\gamma_0}{p_0 + E_p - \mathrm{i}0}\,, \tag{28}$$

where

$$\Lambda^\pm(\mathbf{p}) = \frac{1}{2}\,(1 \pm \gamma_0 \sin\varphi_p \pm \boldsymbol{\alpha}\hat{\mathbf{p}} \cos\varphi_p)\,. \tag{29}$$

The pole of the dressed quark is given by the value E_p ($-E_p$ for the antiquark), which in turn depends on the mass operator, and we thus arrive at a closed system of equations,

$$\begin{aligned} \mathrm{i}\Sigma(\mathbf{p}) &= \int \frac{\mathrm{d}^4 k}{(2\pi)^4}\, V(\mathbf{p}-\mathbf{k})\,\gamma_0\, \frac{1}{S_0^{-1}(k_0, \mathbf{k}) - \Sigma(\mathbf{k})}\,\gamma_0\,, \\ S_0(p_0, \mathbf{p}) &= \frac{1}{\gamma_0 p_0 - \boldsymbol{\gamma}\,\mathbf{p} - m + \mathrm{i}0}\,. \end{aligned} \tag{30}$$

Since the Fourier transform of the potential is independent of energy (which is a consequence of the instantaneous form of the interaction), the integral over the temporal component of the momentum in mass operator (27) only touches upon propagator (28) and can therefore be evaluated explicitly, which in turn allows parameterizing the mass operator in the form

$$\Sigma(\mathbf{p}) = (A_p - m) + \boldsymbol{\gamma}\,\hat{\mathbf{p}}(B_p - p)\,, \quad E_p = A_p \sin\varphi_p + B_p \cos\varphi_p\,, \tag{31}$$

and gives the propagator

$$S^{-1}(p_0, \mathbf{p}) = \gamma_0 p_0 - (\boldsymbol{\gamma}\,\hat{\mathbf{p}})\,B_p - A_p\,. \tag{32}$$

The self-consistency condition for such a parameterization is simply the mass-gap equation (14) for the chiral angle.

3. Beyond the Bardeen–Cooper–Schrieffer level. Mesonic states

In the preceding section, the GNJL model was studied in the BCS approximation with the dressed quarks as the physical degrees of freedom. This approximation allows the phenomenon of spontaneous chiral symmetry breaking in a vacuum to be described microscopically. We note that the model contains confinement and does not therefore support the existence of free quarks. A natural next step is then to proceed beyond the BCS approximation, with the inclusion of the interaction between the dressed quarks and thus with the building of colorless objects — hadrons. In Sections 3.1–3.2, this problem is addressed in the framework of two approaches: in the matrix formalism (see [21–29, 33] for the details) and with the help of a generalized Bogoliubov–Valatin transformation (the relevant details can be found in [33]).

3.1 Bethe–Salpeter equation

In the framework of the matrix formalism, proceeding beyond the BCS approximation is done by considering the Bethe–Salpeter equation for the bound states of quarks and antiquarks, which is written as an equation for the mesonic amplitude $\chi(\mathbf{p}; M)$ in the meson rest frame (where $\mathbf{p}$ is the momentum of the quark and M is the mass of the meson) (Fig. 3),

$$\begin{aligned} \chi(\mathbf{p}; M) = -\mathrm{i} \int \frac{\mathrm{d}^4 q}{(2\pi)^4}\, V(\mathbf{p}-\mathbf{q})\,\gamma_0 S\left(\mathbf{q}, q_0 + \frac{M}{2}\right) \\ \times \chi(\mathbf{q}; M)\, S\left(\mathbf{q}, q_0 - \frac{M}{2}\right)\gamma_0\,. \end{aligned} \tag{33}$$

The instantaneous form of the interaction allows us to simplify this equation considerably. In particular, since the integral for the energy in Eqn (33) only depends on the position of the poles of the propagators, it is easy to see that when the propagators are substituted in the form of Eqn (28), only two terms of the four survive, with the poles in the q_0 complex plane located on different sides of the real axis. The corresponding integrals are then straightforwardly evaluated and give

$$\begin{aligned} \int_{-\infty}^{\infty} \frac{\mathrm{d}q_0}{2\pi\mathrm{i}}\, \frac{1}{q_0 \pm M/2 - E_q + \mathrm{i}0}\, \frac{1}{q_0 \mp M/2 + E_q - \mathrm{i}0} \\ = -\frac{1}{2E_q \mp M}\,, \end{aligned} \tag{34}$$

and hence Eqn (33) becomes the system of coupled equations

$$\begin{aligned} [2E_p - M]\,\chi^{[+]} &= -\int \frac{\mathrm{d}^3 q}{(2\pi)^3}\, V(\mathbf{p}-\mathbf{q})\,\gamma_0 \big[(\Lambda^+\gamma_0)\,\chi^{[+]}(\Lambda^-\gamma_0) \\ &\quad + (\Lambda^-\gamma_0)\,\chi^{[-]}(\Lambda^+\gamma_0)\big]\,\gamma_0\,, \\ [2E_p + M]\,\chi^{[-]} &= -\int \frac{\mathrm{d}^3 q}{(2\pi)^3}\, V(\mathbf{p}-\mathbf{q})\,\gamma_0 \big[(\Lambda^+\gamma_0)\,\chi^{[+]}(\Lambda^-\gamma_0) \\ &\quad + (\Lambda^-\gamma_0)\,\chi^{[-]}(\Lambda^+\gamma_0)\big]\,\gamma_0\,, \end{aligned} \tag{35}$$

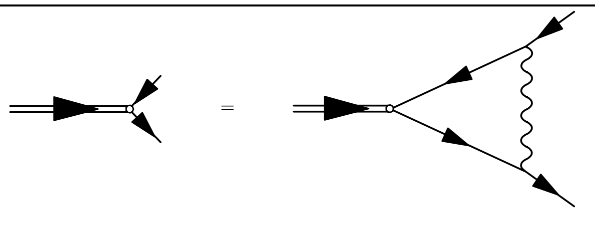

Figure 3. Graphical representation of the Bethe–Salpeter equation for the amplitude $\chi(\mathbf{p}; M)$.

where we introduce the amplitudes

$$\chi^{[+]}(\mathbf{q}; M) = \frac{\chi(\mathbf{q}; M)}{2E_q - M}\,, \quad \chi^{[-]}(\mathbf{q}; M) = \frac{\chi(\mathbf{q}; M)}{2E_q + M}\,.$$

In order to proceed, we

• multiply the first equation in system (35) by $\bar{u}_{s_1}$ from the left and by v_{s_2} from the right, and do the same for the second equation, with $\bar{v}_{s_3}$ and u_{s_4}, respectively;

• represent the projectors $\Lambda^{\pm}$ in terms of bispinors,

$$\Lambda^+(\mathbf{p}) = \sum_s u_s(\mathbf{p}) \otimes u_s^{\dagger}(\mathbf{p})\,,$$
$$\Lambda^-(\mathbf{p}) = \sum_s v_{-s}(-\mathbf{p}) \otimes v_{-s}^{\dagger}(-\mathbf{p})\,; \tag{36}$$

• define matrix amplitudes $\phi^+_{s_1 s_2} = [\bar{u}_{s_1} \chi^{[+]} v_{-s_2}]$ and $\phi^-_{s_1 s_2} = [\bar{v}_{-s_1} \chi^{[-]} u_{s_2}]$.

As a result, the Bethe–Salpeter equation takes the form

$$\left\{ \begin{aligned} &[2E_p - M]\,\phi^+_{s_1 s_2} = -\sum_{s_3 s_4} \int \frac{d^3 q}{(2\pi)^3}\, V(\mathbf{p} - \mathbf{q}) \\ &\quad \times \left\{ [v^{++}]_{s_1 s_2 s_3 s_4} \phi^+_{s_3 s_4} + [v^{+-}]_{s_1 s_2 s_3 s_4} \phi^-_{s_3 s_4} \right\}, \\ &[2E_p + M]\,\phi^-_{s_1 s_2} = -\sum_{s_3 s_4} \int \frac{d^3 q}{(2\pi)^3}\, V(\mathbf{p} - \mathbf{q}) \\ &\quad \times \left\{ [v^{-+}]_{s_1 s_2 s_3 s_4} \phi^+_{s_3 s_4} + [v^{--}]_{s_1 s_2 s_3 s_4} \phi^-_{s_3 s_4} \right\}, \end{aligned} \right. \tag{37}$$

where we define the quantities $v^{\pm\pm}$ such that

$$\begin{aligned} &\left[v^{++}(\mathbf{p}, \mathbf{q})\right]_{s_1 s_3 s_4 s_2} = \left[\bar{u}_{s_1}(\mathbf{p})\, \gamma_0 u_{s_3}(\mathbf{q})\right] \left[\bar{v}_{-s_4}(-\mathbf{q})\, \gamma_0 v_{-s_2}(-\mathbf{p})\right], \\ &\left[v^{+-}(\mathbf{p}, \mathbf{q})\right]_{s_1 s_3 s_4 s_2} = \left[\bar{u}_{s_1}(\mathbf{p})\, \gamma_0 v_{-s_3}(-\mathbf{q})\right] \left[\bar{u}_{s_4}(\mathbf{q})\, \gamma_0 v_{-s_2}(-\mathbf{p})\right], \\ &\left[v^{-+}(\mathbf{p}, \mathbf{q})\right]_{s_1 s_3 s_4 s_2} = \left[\bar{v}_{-s_1}(-\mathbf{p})\, \gamma_0 u_{s_3}(\mathbf{q})\right] \left[\bar{v}_{-s_4}(-\mathbf{q})\, \gamma_0 u_{s_2}(\mathbf{p})\right], \\ &\left[v^{--}(\mathbf{p}, \mathbf{q})\right]_{s_1 s_3 s_4 s_2} = \left[\bar{v}_{-s_1}(-\mathbf{p})\, \gamma_0 v_{-s_3}(-\mathbf{q})\right] \left[\bar{u}_{s_4}(\mathbf{q})\, \gamma_0 u_{s_2}(\mathbf{p})\right], \end{aligned} \tag{38}$$

with

$$\begin{aligned} &\left[\bar{u}_s(\mathbf{k}_1)\, \gamma_0 u_{s'}(\mathbf{k}_2)\right] = \left[C_{k_1} C_{k_2} + S_{k_1} S_{k_2} (\boldsymbol{\sigma}\hat{\mathbf{k}}_1)(\boldsymbol{\sigma}\hat{\mathbf{k}}_2)\right]_{s,s'}, \\ &\left[\bar{v}_{-s}(-\mathbf{k}_1)\, \gamma_0 v_{-s'}(-\mathbf{k}_2)\right] = \left[(-\mathrm{i}\sigma_2)\big(C_{k_1} C_{k_2} \right. \\ &\qquad \left. + S_{k_1} S_{k_2} (\boldsymbol{\sigma}\hat{\mathbf{k}}_1)(\boldsymbol{\sigma}\hat{\mathbf{k}}_2)\big)(\mathrm{i}\sigma_2)\right]_{s,s'}, \\ &\left[\bar{v}_{-s}(-\mathbf{k}_1)\, \gamma_0 u_{s'}(\mathbf{k}_2)\right] = \left[\big(S_{k_1} C_{k_2} (\boldsymbol{\sigma}\hat{\mathbf{k}}_1) \right. \\ &\qquad \left. - S_{k_2} C_{k_1} (\boldsymbol{\sigma}\hat{\mathbf{k}}_2)\big)(\mathrm{i}\sigma_2)\right]_{s,s'}, \\ &\left[\bar{u}_s(\mathbf{k}_1)\, \gamma_0 v_{-s'}(-\mathbf{k}_2)\right] = -\left[(\mathrm{i}\sigma_2)\big(S_{k_1} C_{k_2} (\boldsymbol{\sigma}\hat{\mathbf{k}}_1) \right. \\ &\qquad \left. - S_{k_2} C_{k_1} (\boldsymbol{\sigma}\hat{\mathbf{k}}_2)\big)\right]_{s,s'}, \end{aligned} \tag{39}$$

and where the following shorthand notation is used:

$$\begin{aligned} C_p &= \cos\left[\frac{1}{2}\left(\frac{\pi}{2} - \varphi_p\right)\right] = \sqrt{\frac{1 + \sin\varphi_p}{2}}\,, \\ S_p &= \sin\left[\frac{1}{2}\left(\frac{\pi}{2} - \varphi_p\right)\right] = \sqrt{\frac{1 - \sin\varphi_p}{2}}\,. \end{aligned} \tag{40}$$

It is also convenient to include the potential in the definition of the amplitudes, thus writing

$$\begin{aligned} \left[T^{++}(\mathbf{p}, \mathbf{q})\right]_{s_1 s_3 s_4 s_2} &= \left[\bar{u}_{s_1}(\mathbf{p})\, \gamma_0 u_{s_3}(\mathbf{q})\right] \left[-V(\mathbf{p} - \mathbf{q})\right] \\ &\quad \times \left[\bar{v}_{-s_4}(-\mathbf{q})\, \gamma_0 v_{-s_2}(-\mathbf{p})\right], \\ \left[T^{+-}(\mathbf{p}, \mathbf{q})\right]_{s_1 s_3 s_4 s_2} &= \left[\bar{u}_{s_1}(\mathbf{p})\, \gamma_0 v_{-s_3}(-\mathbf{q})\right] \left[-V(\mathbf{p} - \mathbf{q})\right] \\ &\quad \times \left[\bar{u}_{s_4}(\mathbf{q})\, \gamma_0 v_{-s_2}(-\mathbf{p})\right], \\ \left[T^{-+}(\mathbf{p}, \mathbf{q})\right]_{s_1 s_3 s_4 s_2} &= \left[\bar{v}_{-s_1}(-\mathbf{p})\, \gamma_0 u_{s_3}(\mathbf{q})\right] \left[-V(\mathbf{p} - \mathbf{q})\right] \\ &\quad \times \left[\bar{v}_{-s_4}(-\mathbf{q})\, \gamma_0 v_{-s_2}(\mathbf{p})\right], \\ \left[T^{--}(\mathbf{p}, \mathbf{q})\right]_{s_1 s_3 s_4 s_2} &= \left[\bar{v}_{-s_1}(-\mathbf{p})\, \gamma_0 v_{-s_3}(-\mathbf{q})\right] \\ &\quad \times \left[-V(\mathbf{p} - \mathbf{q})\right] \left[\bar{u}_{s_4}(\mathbf{q})\, \gamma_0 u_{s_2}(\mathbf{p})\right], \end{aligned} \tag{41}$$

or, symbolically,

$$\begin{aligned} &T^{++} = [\bar{u}\gamma_0 u][-V][\bar{v}\gamma_0 v]\,, \quad T^{+-} = [\bar{u}\gamma_0 v][-V][\bar{u}\gamma_0\, v]\,, \\ &T^{-+} = [\bar{v}\gamma_0 u][-V][\bar{v}\gamma_0 u]\,, \quad T^{--} = [\bar{v}\gamma_0 v][-V][\bar{u}\gamma_0 u]\,. \end{aligned} \tag{42}$$

Equations (37) comprise the Bethe–Salpeter equation in the so-called energy–spin formalism described in [25–29].

In [16], the approach of matrix wave functions is suggested for the two-dimensional QCD, which is convenient in various applications. Below, this approach is generalized to the four-dimensional GNJL model [33].

To begin, we note that it is convenient to define the Foldy operator T_p and use it to rewrite the Dirac projectors $\Lambda^{\pm}$ in (29):

$$\begin{aligned} &\Lambda^{\pm}(\mathbf{p}) = T_p P_{\pm} T_p^{\dagger}\,, \quad P_{\pm} = \frac{1 \pm \gamma_0}{2}\,, \\ &T_p = \exp\left[-\frac{1}{2}\,\boldsymbol{\gamma}\,\hat{\mathbf{p}}\left(\frac{\pi}{2} - \varphi_p\right)\right]. \end{aligned} \tag{43}$$

As the next step, Eqn (33) for the mesonic amplitude is rewritten in terms of the matrix wave function

$$\tilde{\phi}(\mathbf{p}; M_\pi) = \int \frac{dp_0}{2\pi}\, S\left(\mathbf{p}, p_0 + \frac{M_\pi}{2}\right) \chi(\mathbf{p}; M_\pi)\, S\left(\mathbf{p}, p_0 - \frac{M_\pi}{2}\right), \tag{44}$$

which is subject to rotation with the Foldy operator T_p both from the left and from the right; we thus define $\phi(\mathbf{p}; M_\pi) = T_p^{\dagger} \tilde{\phi}(\mathbf{p}; M_\pi)\, T_p^{\dagger}$. For such a matrix wave function, Bethe–Salpeter equation (33) takes the form

$$\begin{aligned} \phi(\mathbf{p}; M_\pi) = &-\int \frac{d^3 q}{(2\pi)^3}\, V(\mathbf{p} - \mathbf{q}) \left(P_+\, \frac{T_p^{\dagger} T_q \phi(\mathbf{q}; M_\pi)\, T_q T_p^{\dagger}}{2E_p - M_\pi}\, P_- \right. \\ &\left. + P_-\, \frac{T_p^{\dagger} T_q \phi(\mathbf{q}; M_\pi)\, T_q T_p^{\dagger}}{2E_p + M_\pi}\, P_+ \right). \end{aligned} \tag{45}$$

It is easy to see that the solution of Eqn (45) has the form

$$\phi(\mathbf{p}; M_\pi) = P_+ \mathcal{A} P_- + P_- \mathcal{B} P_+\,, \tag{46}$$

where $\mathcal{A}$ and $\mathcal{B}$ are two unknown matrix functions, which can be expanded in the complete set of the 4×4 matrices, $\{1, \gamma_\mu, \gamma_5, \gamma_\mu\gamma_5, \sigma_{\mu\nu}\}$. We note, however, that due to the orthogonality properties of the projectors $P_+ P_- = P_- P_+ = 0$ and also because the matrix γ_0 can always be absorbed into their definition, the actual set of matrices is reduced to just two, $\{\gamma_5, \boldsymbol{\gamma}\}$, and hence wave function (46) can be represented as

$$\phi(\mathbf{p}; M) = \begin{pmatrix} 0 & \varphi^+(\mathbf{p}) \\ \varphi^-(\mathbf{p}) & 0 \end{pmatrix}, \tag{47}$$

where $\varphi^\pm(\mathbf{p})$ are 2×2 matrices. It is a straightforward exercise to demonstrate that the eigenvalue problem given by (37) is equivalent to the one given by (45), with

$$\phi^+_{s_1 s_2} = \mathrm{i}(\varphi^+\sigma_2)_{s_1 s_2}\,, \quad \phi^-_{s_1 s_2} = \mathrm{i}(\sigma_2\varphi^-)_{s_1 s_2}\,. \tag{48}$$

Further transformations correspond to projecting the matrix amplitudes onto the states with the given total momentum and spatial and charge parities.

3.2 Chiral pion

We first consider the case of a chiral pion. For the corresponding matrix amplitude, we have

$$\phi^\pm_{s_1 s_2}(\mathbf{p}) = \left[\frac{\mathrm{i}}{\sqrt{2}}\,\sigma_2\right]_{s_1 s_2} Y_{00}(\hat{\mathbf{p}})\,\varphi^\pm_\pi(p)\,, \tag{49}$$

where $Y_{00}(\hat{\mathbf{p}}) = 1/\sqrt{4\pi}$ is the lowest spherical harmonic normalized to unity. Then, if the amplitudes $T^{\pm\pm}_\pi(p,q)$ are introduced in accordance with Eqn (41) and all spin traces are taken explicitly, we arrive at the following system of equations for the scalar wave functions $\varphi^\pm_\pi$:

$$\begin{aligned} &[2E_p - M_\pi]\,\varphi^+_\pi(p) \\ &\quad = \int \frac{q^2\,\mathrm{d}q}{(2\pi)^3}\left[T^{++}_\pi(p,q)\,\varphi^+_\pi(q) + T^{+-}_\pi(p,q)\,\varphi^-_\pi(q)\right], \\ &[2E_p + M_\pi]\,\varphi^-_\pi(p) \\ &\quad = \int \frac{q^2\,\mathrm{d}q}{(2\pi)^3}\left[T^{-+}_\pi(p,q)\,\varphi^+_\pi(q) + T^{--}_\pi(p,q)\,\varphi^-_\pi(q)\right], \end{aligned} \tag{50}$$

where

$$\begin{aligned} T^{++}_\pi(p,q) &= T^{--}_\pi(p,q) = -\int \mathrm{d}\Omega_q V(\mathbf{p}-\mathbf{q}) \\ &\quad\times\left(\cos^2\frac{\varphi_p - \varphi_q}{2} - \frac{1-\hat{\mathbf{p}}\hat{\mathbf{q}}}{2}\cos\varphi_p\cos\varphi_q\right), \\ T^{+-}_\pi(p,q) &= T^{-+}_\pi(p,q) = -\int \mathrm{d}\Omega_q V(\mathbf{p}-\mathbf{q}) \\ &\quad\times\left(\sin^2\frac{\varphi_p - \varphi_q}{2} + \frac{1-\hat{\mathbf{p}}\hat{\mathbf{q}}}{2}\cos\varphi_p\cos\varphi_q\right). \end{aligned} \tag{51}$$

The resulting system of equations (50) can be interpreted as a bound-state equation for a quark–antiquark pair in the channel with quantum numbers of the pion. The physical interpretation of the two amplitudes used to describe one meson comes from the observation that the quark–antiquark pair in it can move both forward and backward in time, and each type of motion is described by an independent amplitude [16, 21–29]. Thus, the Hamiltonian turns out to be a matrix in the so-called energy–spin space, and the bound-state equation takes the form of a system of two coupled equations.

It can be verified explicitly that in the strict chiral limit $m = 0$, the function

$$\varphi^+_\pi(p) = \varphi^-_\pi(p) = \sin\varphi_p \tag{52}$$

is a solution of system (50) with the eigenvalue $M_\pi = 0$. Indeed, substituting function (52) and $M_\pi = 0$ in system (50), we arrive at the single equation

$$\begin{aligned} 2E_p\varphi_\pi(p) &= \int \frac{q^2\,\mathrm{d}q}{(2\pi)^3}\left(T^{++}_\pi(p,q) + T^{+-}_\pi(p,q)\right)\varphi_\pi(q) \\ &= -\int \frac{\mathrm{d}^3 q}{(2\pi)^3}\,V(\mathbf{p}-\mathbf{q})\,\varphi_\pi(q)\,, \end{aligned} \tag{53}$$

which holds due to mass-gap equation (14) and dispersive law (15). The resulting equation looks especially simple and instructive in the coordinate space:

$$\left(2E_p + V(r)\right)\varphi_\pi = 0\,. \tag{54}$$

Formally, it takes the form of a simple Salpeter equation with equal masses and with the eigenvalue $M = 0$; however, the form of the quantity E_p is very different from the simple kinetic energy of a free quark $(p^2 + m^2)^{1/2}$, which guarantees the existence of the vanishing eigenvalue.

We show in such a way that in the chiral limit, the pion Bethe–Salpeter equation is equivalent to the mass-gap equation for the chiral angle, which, in turn, demonstrates the celebrated dualism of the pion: as a Goldstone boson, it already appears at the BCS level, while beyond the BCS description the same pion emerges from the Bethe–Salpeter equation, as the lowest level in the spectrum of quark–antiquark states.

System of equations (50) allows studying the behavior of the pionic solution near the chiral limit. In particular, it can be demonstrated that as $M_\pi \to 0$, the solution of this system takes the form (higher-order terms in the pion mass are ignored)

$$\begin{aligned} \varphi^\pm_\pi(p) &= \frac{\sqrt{2\pi N_\mathrm{c}}}{f_\pi}\left[\frac{1}{\sqrt{M_\pi}}\sin\varphi_p \pm \sqrt{M_\pi}\varDelta_p\right], \\ f^2_\pi &= \frac{N_\mathrm{c}}{\pi^2}\int_0^\infty p^2\,\mathrm{d}p\varDelta_p\sin\varphi_p\,, \end{aligned} \tag{55}$$

where the function $\varDelta_p$ satisfies an equation that does not contain M_π any more (see also [25–29]):

$$\begin{aligned} 2E_p\varDelta_p &= \sin\varphi_p + \int \frac{\mathrm{d}^3 k}{(2\pi)^3}\,V(\mathbf{p}-\mathbf{k}) \\ &\quad\times\left(\sin\varphi_p\sin\varphi_k + \hat{\mathbf{p}}\hat{\mathbf{k}}\cos\varphi_p\cos\varphi_k\right)\varDelta_k\,. \end{aligned} \tag{56}$$

It is easy to verify that the normalization condition for the wave functions $\varphi^\pm_\pi$ takes the form

$$\int \frac{p^2\,\mathrm{d}p}{(2\pi)^3}\left[\varphi^{+2}_\pi(p) - \varphi^{-2}_\pi(p)\right] = 1\,. \tag{57}$$

The physical interpretation of such a normalization becomes clear from the generalized Bogoliubov–Valatin transformation for mesonic operators.

We now consider the matrix structure of the pionic wave function. In the case of the pion, it is obvious that only γ_5 contributes, and we can therefore extract the matrix structure of the quantities $\mathcal{A}$ and $\mathcal{B}$ explicitly and introduce the scalar wave functions $\varphi^\pm_\pi$ as

$$\mathcal{A}_\pi = \gamma_5\varphi^+_\pi(p)\,, \quad \mathcal{B}_\pi = \gamma_5\varphi^-_\pi(p)\,, \tag{58}$$

where the signs and the coefficients are chosen so as to comply with definition (49) used previously. Thus, with the help of

Eqns (46) and (58), it is easy to see that the pion wave function becomes

$$\tilde{\phi}(\mathbf{p}; M_\pi) = T_p\left[P_+\gamma_5\varphi_\pi^+ + P_-\gamma_5\varphi_\pi^-\right] T_p = \gamma_5 G_\pi + \gamma_0\gamma_5 T_p^2 F_\pi\,, \tag{59}$$

where $G_\pi = (1/2)\,(\varphi_\pi^+ + \varphi_\pi^-)$ and $F_\pi = (1/2)(\varphi_\pi^+ - \varphi_\pi^-)$, and Bethe–Salpeter equation (45) can be rewritten in the form

$$\begin{aligned} M_\pi\tilde{\phi}(\mathbf{p}; M_\pi) &= (\boldsymbol{\alpha}\mathbf{p} + \gamma_0 m)\,\tilde{\phi}(\mathbf{p}; M_\pi) \\ &+ \tilde{\phi}(\mathbf{p}; M_\pi)(\boldsymbol{\alpha}\mathbf{p} - \gamma_0 m) + \int \frac{\mathrm{d}^3 q}{(2\pi)^3}\, V(\mathbf{p}-\mathbf{q}) \\ &\times \big(\Lambda^+(\mathbf{q})\,\tilde{\phi}(\mathbf{p}; M_\pi)\,\Lambda^-(-\mathbf{q}) - \Lambda^+(\mathbf{p})\,\tilde{\phi}(\mathbf{q}; M_\pi)\,\Lambda^-(-\mathbf{p}) \\ &- \Lambda^-(\mathbf{q})\,\tilde{\phi}(\mathbf{p}; M_\pi)\,\Lambda^+(-\mathbf{q}) + \Lambda^-(\mathbf{p})\,\tilde{\phi}(\mathbf{q}; M_\pi)\,\Lambda^+(-\mathbf{p})\big). \end{aligned} \tag{60}$$

Multiplying the last equation by $\gamma_0\gamma_5$, integrating it over the momentum $\mathbf{p}$, and taking the trace in the spin matrices, we arrive at the relation

$$M_\pi \int \frac{\mathrm{d}^3 p}{(2\pi)^3}\, F_\pi \sin\varphi_p = 2m \int \frac{\mathrm{d}^3 p}{(2\pi)^3}\, G_\pi\,, \tag{61}$$

which can easily be identified as the celebrated Gell-Mann–Oakes–Renner relation, if the explicit form of pion wave function (55) is used together with the quantities G_π and F_π, defined as

$$G_\pi = \frac{\sqrt{2\pi N_c}}{f_\pi\sqrt{M_\pi}}\sin\varphi_p\,, \quad F_\pi = \frac{\sqrt{2\pi M_\pi N_c}}{f_\pi}\,\Delta_p\,, \tag{62}$$

with the pion decay constant f_π and the function Δ_p introduced in Eqn (55). Then the conventional form of the Gell-Mann–Oakes–Renner relation [45] is readily restored as soon as formula (24) for the chiral condensate is used:

$$f_\pi^2 M_\pi^2 = -2m\langle\bar{\psi}\psi\rangle\,. \tag{63}$$

3.3 Bogoliubov transformation for mesonic operators

In [53], an alternative approach to mesonic states in the two-dimensional model for QCD was proposed, allowing the study of mesonic states in this theory with the help of the generalized Bogoliubov–Valatin transformation for the mesonic sector. This approach can naturally be generalized to the four-dimensional GNJL model. Such a generalization, suggested in [33], is described in detail below.

We define four operators quadratic in the quark operators. Among them, the first two,

$$\begin{aligned} \hat{B}_{ss'}(\mathbf{p},\mathbf{p}') &= \frac{1}{\sqrt{N_c}}\sum_\alpha \hat{b}^\dagger_{\alpha s}(\mathbf{p})\,\hat{b}_{\alpha s'}(\mathbf{p}')\,, \\ \hat{D}_{ss'}(\mathbf{p},\mathbf{p}') &= \frac{1}{\sqrt{N_c}}\sum_\alpha \hat{d}^\dagger_{\alpha s}(-\mathbf{p})\,\hat{d}_{\alpha s'}(-\mathbf{p}')\,, \end{aligned} \tag{64}$$

'count' the number of quarks and antiquarks, while the other two,

$$\begin{aligned} \hat{M}^\dagger_{ss'}(\mathbf{p},\mathbf{p}') &= \frac{1}{\sqrt{N_c}}\sum_\alpha \hat{b}^\dagger_{\alpha s'}(\mathbf{p}')\,\hat{d}^\dagger_{\alpha s}(-\mathbf{p})\,, \\ \hat{M}_{ss'}(\mathbf{p},\mathbf{p}') &= \frac{1}{\sqrt{N_c}}\sum_\alpha \hat{d}_{\alpha s}(-\mathbf{p})\,\hat{b}_{\alpha s'}(\mathbf{p}')\,, \end{aligned} \tag{65}$$

create and annihilate quark–antiquark pairs. In the limit $N_c \to \infty$, the introduced operators obey the standard bosonic commutation relations. In particular, the only nonvanishing commutator is

$$\begin{aligned} &\left[\hat{M}_{ss'}(\mathbf{p},\mathbf{p}')\ \hat{M}^\dagger_{\sigma\sigma'}(\mathbf{q},\mathbf{q}')\right] \\ &\quad = (2\pi)^3\delta^{(3)}(\mathbf{p}-\mathbf{q})(2\pi)^3\delta^{(3)}(\mathbf{p}'-\mathbf{q}')\,\delta_{s\sigma}\delta_{s'\sigma'}\,. \end{aligned} \tag{66}$$

It is easy to see that at the BCS level, Hamiltonian (18) is expressed entirely in terms of the first pair of the above operators,

$$\hat{H} = E_{\mathrm{vac}} + \sqrt{N_c}\sum_{s=\uparrow,\downarrow}\int \frac{\mathrm{d}^3 p}{(2\pi)^3}\,E_p\big(\hat{B}_{ss}(\mathbf{p},\mathbf{p}) + \hat{D}_{ss}(\mathbf{p},\mathbf{p})\big]\,, \tag{67}$$

while the omitted part (at the BCS level, suppressed in the large-N_c limit) of the Hamiltonian $:\hat{H}_4:$ contains all four operators. The key observation of the approach is the statement that in the presence of confinement, quarks and antiquarks cannot be created or annihilated as isolated objects — this is only possible for quark–antiquark pairs. Therefore, beyond the BCS approximation, operators (64) cannot be independent, but must be expressed in terms of operators (65). In the large-N_c limit, it is sufficient to restrict to the minimal number of quark–antiquark pairs, that is, to retain only one accompanying antiquark for each created quark and vice versa and not to consider the entire quark–antiquark cloud. Then the sought relation between the operators is

$$\begin{aligned} \hat{B}_{ss'}(\mathbf{p},\mathbf{p}') &= \frac{1}{\sqrt{N_c}}\sum_{s''}\int \frac{\mathrm{d}^3 p''}{(2\pi)^3}\,\hat{M}^\dagger_{s''s}(\mathbf{p}'',\mathbf{p})\,\hat{M}_{s''s'}(\mathbf{p}'',\mathbf{p}')\,, \\ \hat{D}_{ss'}(\mathbf{p},\mathbf{p}') &= \frac{1}{\sqrt{N_c}}\sum_{s''}\int \frac{\mathrm{d}^3 p''}{(2\pi)^3}\,\hat{M}^\dagger_{ss''}(\mathbf{p},\mathbf{p}'')\hat{M}_{s's''}(\mathbf{p}',\mathbf{p}''). \end{aligned} \tag{68}$$

It is easy to verify that in the limit $N_c \to \infty$, substitution (68) reproduces the commutation relations between operators (64), and it can therefore be interpreted as an independent solution of the equations given by these commutation relations.

If relations (68) are substituted in Hamiltonian (9), the terms $:\hat{H}_2:$ and $:\hat{H}_4:$ turn out to be of the same order of magnitude, while all other terms, suppressed in the limit $N_c \to \infty$, can be disregarded. Then the center-of-mass Hamiltonian of the quark–antiquark cloud takes the form

$$\hat{H} = E'_{\mathrm{vac}} + \int \frac{\mathrm{d}^3 P}{(2\pi)^3}\,\mathcal{H}(\mathbf{P})\,, \tag{69}$$

where (for simplicity, the Hamiltonian density $\mathcal{H}$ is taken in the rest frame, with $\mathbf{P} = 0$)

$$\begin{aligned} \mathcal{H} \equiv \mathcal{H}(\mathbf{P}=0) &= \sum_{s_1 s_2}\int \frac{\mathrm{d}^3 p}{(2\pi)^3}\,2E_p\hat{M}^\dagger_{s_1 s_2}(\mathbf{p},\mathbf{p})\,\hat{M}_{s_2 s_1}(\mathbf{p},\mathbf{p}) \\ &+ \frac{1}{2}\sum_{s_1 s_2 s_3 s_4}\int \frac{\mathrm{d}^3 p}{(2\pi)^3}\frac{\mathrm{d}^3 q}{(2\pi)^3}\,V(\mathbf{p}-\mathbf{q}) \\ &\times \Big\{\left[v^{++}(\mathbf{p},\mathbf{q})\right]_{s_1 s_3 s_4 s_2}\hat{M}^\dagger_{s_2 s_1}(\mathbf{p},\mathbf{p})\,\hat{M}_{s_4 s_3}(\mathbf{q},\mathbf{q}) \\ &+ \left[v^{+-}(\mathbf{p},\mathbf{q})\right]_{s_1 s_3 s_4 s_2}\hat{M}^\dagger_{s_2 s_1}(\mathbf{q},\mathbf{q})\,\hat{M}^\dagger_{s_3 s_4}(\mathbf{p},\mathbf{p}) \\ &+ \left[v^{-+}(\mathbf{p},\mathbf{q})\right]_{s_1 s_3 s_4 s_2}\hat{M}_{s_1 s_2}(\mathbf{p},\mathbf{p})\,\hat{M}_{s_4 s_3}(\mathbf{q},\mathbf{q}) \\ &+ \left[v^{--}(\mathbf{p},\mathbf{q})\right]_{s_1 s_3 s_4 s_2}\hat{M}_{s_3 s_4}(\mathbf{p},\mathbf{p})\,\hat{M}^\dagger_{s_1 s_2}(\mathbf{q},\mathbf{q})\Big\}\,, \end{aligned} \tag{70}$$

and the amplitudes v are given by the expressions in Eqn (38).

Strictly speaking, only two amplitudes of the four in Eqn (38), for example, v^{++} and v^{+-}, are independent, while the others, v^{--} and v^{-+}, are related to them by the operation of Hermitian conjugation. Nevertheless, we prefer to keep all four amplitudes explicitly in order to preserve the most symmetric form of the equations.

3.3.1 The case of the chiral pion. Before we come to the diagonalization of the full Hamiltonian (70), we treat the case of the chiral pion separately. For the pion, $J = L = S = 0$, and hence the operator $\hat{M}_{ss'}(\mathbf{p},\mathbf{p})$ can be written in the form

$$\hat{M}_{ss'}(\mathbf{p},\mathbf{p}) = \left[\frac{\mathrm{i}}{\sqrt{2}}\,\sigma_2 Y_{00}(\hat{\mathbf{p}})\right]_{ss'} \hat{M}(p)\,, \tag{71}$$

where the spin–angular structure is equivalent to the one in the matrix wave function of the pion, Eqn (49).

Substituting expression (71) in Hamiltonian (70), we find

$$\begin{aligned}\hat{\mathcal{H}}_\pi = \int \frac{p^2\,\mathrm{d}p}{(2\pi)^3}\, 2E_p \hat{M}^\dagger(p)\,\hat{M}(p) - \frac{1}{2}\int \frac{p^2\,\mathrm{d}p}{(2\pi)^3}\,\frac{q^2\,\mathrm{d}q}{(2\pi)^3} \\ \times \big(T_\pi^{++}(p,q)\,\hat{M}^\dagger(p)\,M(q) + T_\pi^{+-}(p,q)\,\hat{M}^\dagger(q)\,\hat{M}^\dagger(p) \\ + T_\pi^{-+}(p,q)\,\hat{M}(p)\,\hat{M}(q) + T_\pi^{--}(p,q)\,\hat{M}^\dagger(q)\,\hat{M}(p)\big)\,,\end{aligned} \tag{72}$$

where the amplitudes $T_\pi^{\pm\pm}(p,q)$ are nothing more than combinations of the amplitudes $v^{\pm\pm}(\mathbf{p},\mathbf{q})$ and the potential $V(\mathbf{p}-\mathbf{q})$, integrated with respect to the angle [see Eqn (51)].

Expression (72) is a typical Hamiltonian requiring diagonalization by a bosonic Bogoliubov–Valatin transformation of the form

$$\begin{aligned}\hat{M}(p) &= \hat{m}_\pi \varphi_\pi^+(p) + \hat{m}_\pi^\dagger \varphi_\pi^-(p)\,,\\ \hat{M}^\dagger(p) &= \hat{m}_\pi^\dagger \varphi_\pi^+(p) + \hat{m}_\pi \varphi_\pi^-(p)\,,\end{aligned} \tag{73}$$

which can be inverted as

$$\begin{aligned}\hat{m}_\pi &= \int \frac{p^2\,\mathrm{d}p}{(2\pi)^3}\,\big(\hat{M}(p)\,\varphi_\pi^+(p) - \hat{M}^\dagger(p)\,\varphi_\pi^-(p)\big)\,,\\ \hat{m}_\pi^\dagger &= \int \frac{p^2\,\mathrm{d}p}{(2\pi)^3}\,\big(\hat{M}^\dagger(p)\,\varphi_\pi^+(p) - \hat{M}(p)\,\varphi_\pi^-(p)\big)\,.\end{aligned} \tag{74}$$

The operators $\hat{m}_\pi^\dagger$ and $\hat{m}_\pi$ support a clear physical interpretation: they create and annihilate the pion in its rest frame. Then, with the help of the commutator

$$\big[\hat{M}(p),\, \hat{M}^\dagger(q)\big] = \frac{(2\pi)^3}{p^2}\,\delta(p-q)\,, \tag{75}$$

which follows directly from Eqn (66), it is straightforward to find that

$$\big[\hat{m}_\pi,\, \hat{m}_\pi^\dagger\big] = \int \frac{p^2\,\mathrm{d}p}{(2\pi)^3}\,\big(\varphi_\pi^{+2}(p) - \varphi_\pi^{-2}(p)\big)\,. \tag{76}$$

Therefore, the requirement of the canonical commutation relation between the bosonic creation and annihilation operators for the pion, $[\hat{m}_\pi, \hat{m}_\pi^\dagger] = 1$, leads to the normalization condition (amplitudes $\varphi_\pi^\pm(p)$ are chosen real) of form (57), which is just the standard condition for the Bogoliubov amplitudes. At the same time, the equation that guarantees cancellation of the anomalous Bogoliubov terms in Hamiltonian (72), that is, that $\langle\Omega|\hat{\mathcal{H}}_\pi|\pi\pi\rangle = 0$ and $\langle\pi\pi|\hat{\mathcal{H}}_\pi|\Omega\rangle = 0$ (where $|\Omega\rangle$ is the vacuum annihilated by the mesonic operators, for example, $\hat{m}_\pi$), takes the form of the bound-state equation for the amplitudes $\varphi_\pi^\pm(p)$ [see Eqn (50)].

It is important to note that the vacuum $|\Omega\rangle$ annihilated by the operator $\hat{m}_\pi$ differs from the BCS vacuum $|0\rangle$ and both vacua are related by a unitary transformation,

$$\hat{m}_\pi|\Omega\rangle = \hat{m}_\pi U^\dagger|0\rangle = U^\dagger(U\hat{m}_\pi U^\dagger)|0\rangle \propto U^\dagger \hat{M}(p)|0\rangle = 0\,.$$

Because the quark–antiquark pair creation is suppressed in the large-N_c limit, the deviation of the operator $U^\dagger$ from unity demonstrates the same suppression pattern. Similarly, the vacuum energy E'_vac in Eqn (69) differs from the vacuum energy E_vac in BCS Hamiltonian (18), and it contains contributions from the commutators of the operators $\hat{M}$ and $\hat{M}^\dagger$ (suppressed in the limit $N_\mathrm{c}\to\infty$). Finally, the chiral condensate evaluated in the BCS approximation provides the leading-order term in the expansion of the exact condensate in inverse powers of N_c.

Hamiltonian (72) diagonalized in the given order in N_c takes the form

$$\hat{\mathcal{H}}_\pi = M_\pi \hat{m}_\pi^\dagger \hat{m}_\pi\,, \quad M_\pi = \langle\pi|\hat{\mathcal{H}}_\pi|\pi\rangle\,, \tag{77}$$

where M_π is the pion mass, and the omitted terms (suppressed for large N_c) describe pion–pion scattering.

3.3.2 The general case. We now diagonalize the full Hamiltonian (70) in terms of compound mesonic states. With a trivial generalization of Eqns (73) and (74),

$$\begin{aligned}\hat{M}_{ss'}(\mathbf{p},\mathbf{p}) &= \sum_n \big(\hat{m}_n \phi^+_{n,ss'}(\mathbf{p}) + \hat{m}_n^\dagger \phi^-_{n,ss'}(\mathbf{p})\big)\,,\\ \hat{M}^\dagger_{ss'}(\mathbf{p},\mathbf{p}) &= \sum_n \big(\hat{m}_n^\dagger \phi^{+\dagger}_{n,ss'}(\mathbf{p}) + \hat{m}_n \phi^{-\dagger}_{n,ss'}(\mathbf{p})\big)\,,\end{aligned} \tag{78}$$

$$\begin{aligned}\hat{m}_n &= \int \frac{\mathrm{d}^3p}{(2\pi)^3}\,\mathrm{Sp}\big(\hat{M}(\mathbf{p},\mathbf{p})\,\phi_n^{+\dagger}(\mathbf{p}) - \hat{M}^\dagger(\mathbf{p},\mathbf{p})\,\phi_n^-(\mathbf{p})\big)\,,\\ \hat{m}_n^\dagger &= \int \frac{\mathrm{d}^3p}{(2\pi)^3}\,\mathrm{Sp}\big(\hat{M}^\dagger(\mathbf{p},\mathbf{p})\,\phi_n^+(\mathbf{p}) - \hat{M}(\mathbf{p},\mathbf{p})\,\phi_n^{-\dagger}(\mathbf{p})\big)\,,\end{aligned} \tag{79}$$

it is straightforward to find the following expressions for the commutators $\hat{m}_n$ and $\hat{m}_m^\dagger$:

$$\begin{aligned}[\hat{m}_n,\, \hat{m}_m^\dagger] &= \int \frac{\mathrm{d}^3p}{(2\pi)^3}\,\mathrm{Sp}\big(\phi_n^{+\dagger}(\mathbf{p})\,\phi_m^+(\mathbf{p}) - \phi_m^{-\dagger}(\mathbf{p})\,\phi_n^-(\mathbf{p})\big)\,,\\ [\hat{m}_n,\, \hat{m}_m] &= \int \frac{\mathrm{d}^3p}{(2\pi)^3}\,\mathrm{Sp}\big(\phi_n^{+\dagger}(\mathbf{p})\,\phi_m^-(\mathbf{p}) - \phi_m^{+\dagger}(\mathbf{p})\,\phi_n^-(\mathbf{p})\big)\,.\end{aligned} \tag{80}$$

Here, the subscripts n and m denote the complete set of quantum numbers describing mesonic states. The natural requirement that $[\hat{m}_n,\, \hat{m}_m^\dagger] = \delta_{mn}$ and $[\hat{m}_n,\, \hat{m}_m] = 0$ leads to the orthogonality condition for the wave functions in the form

$$\begin{aligned}&\int \frac{\mathrm{d}^3p}{(2\pi)^3}\,\mathrm{Sp}\big(\phi_n^{+\dagger}(\mathbf{p})\,\phi_m^+(\mathbf{p}) - \phi_m^{-\dagger}(\mathbf{p})\,\phi_n^-(\mathbf{p})\big) = \delta_{nm}\,,\\ &\int \frac{\mathrm{d}^3p}{(2\pi)^3}\,\mathrm{Sp}\big(\phi_n^{+\dagger}(\mathbf{p})\,\phi_m^-(\mathbf{p}) - \phi_m^{+\dagger}(\mathbf{p})\,\phi_n^-(\mathbf{p})\big) = 0\,.\end{aligned} \tag{81}$$

It is then easy to verify that representation (78), together with the orthogonality and normalisation condition (81), guarantees that the Hamiltonian is diagonal, that is,

$$\hat{\mathcal{H}} = \sum_n M_n m_n^\dagger m_n + O\left(\frac{1}{\sqrt{N_c}}\right), \tag{82}$$

if the mesonic wave functions $\phi^{\pm}_{n,s_1 s_2}$ satisfy system of equations (37) with the eigenvalue $M = M_n$.

In the leading order in N_c, Hamiltonian (82) describes stable mesons, while the neglected (N_c-suppressed) terms include quark exchanges and therefore describe decays and scattering of the mesons (see review [20], where such suppressed terms are restored for two-dimensional QCD).

In practical applications, the Hamiltonian is diagonalized in the J^{PC} basis. For this, we should keep in mind that while the Hamiltonian commutes with the sum $\mathbf{J} = \mathbf{S} + \mathbf{L}$, it does not commute with either the operator of the total quark spin $\mathbf{S}$ or the operator of the angular momentum $\mathbf{L}$ separately.

The case of spin singlets, $P = (-1)^{J+1}$, and $C = (-1)^J$, is trivial in this respect, because the wave functions are given by the expression

$$\phi^{\pm}_{n,s_1 s_2}(\mathbf{p}) = \left[\frac{\mathrm{i}}{\sqrt{2}}\,\sigma_2\right]_{s_1 s_2} Y_{Jm}(\hat{\mathbf{p}})\,\varphi_n^{\pm}(p)\,, \tag{83}$$

where $Y_{Jm}(\hat{\mathbf{p}})$ is the spherical harmonic with the momentum J and magnetic quantum number m. Spin triplets with $J = L$, $P = (-1)^{J+1}$, and $C = (-1)^{J+1}$ are described by

$$\begin{aligned} \phi^{+}_{n,s_1 s_2}(\mathbf{p}) &= \left[\big(\boldsymbol{\sigma}\mathbf{Y}_{JJm}(\hat{\mathbf{p}})\big)\,\frac{\mathrm{i}}{\sqrt{2}}\,\sigma_2\right]_{s_1 s_2} \varphi_n^{+}(p)\,, \\ \phi^{-}_{n,s_1 s_2}(\mathbf{p}) &= \left[\frac{\mathrm{i}}{\sqrt{2}}\,\sigma_2\big(\boldsymbol{\sigma}\mathbf{Y}_{JJm}(\hat{\mathbf{p}})\big)\right]_{s_1 s_2} \varphi_n^{-}(p)\,, \end{aligned} \tag{84}$$

where $\mathbf{Y}_{Jlm}(\hat{\mathbf{p}})$ is the spherical vector with the total momentum J, the orbital momentum l, and the magnetic quantum number m.

The case $L = J \pm 1$, $P = (-1)^J$, and $C = (-1)^J$ is more complicated, because it has to be described by four scalar amplitudes $\varphi^{\pm}_{J\pm1,n}(p)$ (with the obvious exception of the 0^{++} scalar meson with $J = 0$ and $l = 1$),

$$\begin{aligned} \phi^{+}_{n,s_1 s_2}(\mathbf{p}) &= \left[\big(\boldsymbol{\sigma}\mathbf{Y}_{JJ-1m}(\hat{\mathbf{p}})\big)\,\frac{\mathrm{i}}{\sqrt{2}}\,\sigma_2\right]_{s_1 s_2} \varphi^{+}_{J-1,n}(p) \\ &\quad + \left[\big(\boldsymbol{\sigma}\mathbf{Y}_{JJ+1m}(\hat{\mathbf{p}})\big)\,\frac{\mathrm{i}}{\sqrt{2}}\,\sigma_2\right]_{s_1 s_2} \varphi^{+}_{J+1,n}(p)\,, \\ \phi^{-}_{n,s_1 s_2}(\mathbf{p}) &= \left[\frac{\mathrm{i}}{\sqrt{2}}\,\sigma_2\big(\boldsymbol{\sigma}\mathbf{Y}_{JJ-1m}(\hat{\mathbf{p}})\big)\right]_{s_1 s_2} \varphi^{-}_{J-1,n}(p) \\ &\quad + \left[\frac{\mathrm{i}}{\sqrt{2}}\,\sigma_2\big(\boldsymbol{\sigma}\mathbf{Y}_{JJ+1m}(\hat{\mathbf{p}})\big)\right]_{s_1 s_2} \varphi^{-}_{J+1,n}(p)\,, \end{aligned} \tag{85}$$

and the interaction in system of equations (37) mixes all four amplitudes in (85); after projection onto spin–angular states, this gives rise to four coupled equations for the scalar amplitudes $\varphi^{\pm}_{J\pm1,n}(p)$. This can be exemplified by the ρ-meson: its quantum numbers 1^{--} correspond to two terms, ${}^3S_1$ and ${}^3D_1$, and hence the ρ-meson has to be described by four amplitudes, rather than only the two needed for, say, a 0^{-+} meson. It is instructive to note that system (37) would describe not only the ρ-meson but also a heavier vector meson that is defined by the orthogonal combination of the S and D waves. Thus, the doubling of the number of scalar functions is nothing but a mere consequence of the situation where the wave function of the ρ-meson is 'entangled' with the wave function of its heavier partner.

Wave functions (83)–(85) are written in the *LS* basis; however, the problem of the adequate choice of the basis cannot be solved in general terms, since the mixing pattern of different partial waves with the same quantum numbers is a dynamical problem. The *LS* basis is quite suitable for heavy quarkonia where partial-wave mixing can be treated as a relativistic correction. Another notable exception is provided by the regime of the effective restoration of chiral symmetry in the spectrum of excited mesons (see Section 5 below) filling chiral multiplets and, as a result, having the wave functions strictly fixed by chiral symmetry (see review [54] and the references therein). In [55], a chiral basis is discussed in detail, which provides a much more convenient framework for studies of the spectrum of mesons in the regime of the effectively restored chiral symmetry. However, it has to be pointed out that this chiral basis *per se* cannot solve the problem of the dynamical mixing of different waves; it only refers to particular combinations of such waves corresponding to those multiplets with the restored chiral symmetry.

A final remark is in order here. Bethe–Salpeter equation (37) describes the spectrum of genuine quark–antiquark states. In the limit $N_c \to \infty$, that is, in the limit inherent to the model under study, such states have well-known properties. In particular, as the number of colors grows, the mass of a genuine $\bar{q}q$ state remains nearly constant, while its width tends to zero, since the effects of the light-quark pair creation from the vacuum are suppressed in this limit. As can be seen from Eqn (82), the leading suppressed terms describing the amplitudes of the two-body decays of the mesons behave as $O(1/\sqrt{N_c})$, thus yielding the well-known typical behavior $1/N_c$ for the width of the mesons. This property allows distinguishing genuine quarkonia from dynamically generated objects, for example, from the scalar state $f_0(500)$. Thus, in [56], in the framework of the unitarized chiral perturbation theory, it was demonstrated that in the limit $N_c \to \infty$, the poles that describe the genuine quarkonia indeed behave as explained above. In the meantime, the pole responsible for the $f_0(500)$ (in the cited paper, an obsolete notation $f_0(600)$ is used) demonstrates an entirely different behavior: its real part (mass) grows with N_c, while the N_c-dependence of its width is rather nontrivial and does not follow the $1/N_c$ law. This observation confirms the common belief that the $f_0(500)$ is a result of the strong interaction between mesons in the final state, and therefore describing this state requires going beyond the formalism used above.

4. Lorentz nature of confinement

One of the important issues in the phenomenology of strong interactions is related to the Lorentz nature of the confining interaction. For example, spin-dependent interactions in the quark–antiquark system are very sensitive to the relations between the potentials added to the mass (scalar interaction), to the energy, or to the momentum (vector interaction) (see, e.g., the key papers [57, 58] as well as a series of later studies, like [59–63]). The phenomenology of heavy quarkonia and lattice calculations [64] is more compatible with the spin-dependent potentials that follow from the scalar confinement. Meanwhile, in a theory with scalar confinement, chiral symmetry would be broken explicitly, and that would contradict the idea of its spontaneous breaking (see [65] for a discussion of the possibility of the coexistence of scalar confinement and spontaneous chiral symmetry breaking). To investigate this problem, we consider a heavy–light quarkonium with the heavy quark treated as a static center. This allows us to study the Lorentz nature of the confining potential and some properties of quark–antiquark mesons, avoiding unnecessary technical complications. The spectrum of the heavy–light system should be described by system of equations (37) generalized to the case of two quark flavors. Later, the limit of the static antiquark is to be taken explicitly in Eqns (37). But first, it is helpful to stick to a different approach to the heavy–light quarkonium based on the vacuum background correlators method (see review [14] and the references therein) and to investigate the Lorentz nature of confinement in such a system [59–63]. The motion of a light quark in the field of the static antiquark should be described by a single-particle Dirac-like equation with the interaction with the static center given by an effective potential. The Lorentz nature of this potential can be investigated this way.

We start from the Green's function of such a heavy–light quarkonium $S_{q\bar{Q}}$ taken in the form [60, 62, 63]

$$S_{q\bar{Q}}(x,y)=\frac{1}{N_c}\int D\psi D\psi^\dagger DA_\mu \exp\left[-\frac{1}{4}\int d^4x F_{\mu\nu}^{a2} - \int d^4x\psi^\dagger(-i\hat{\partial}-im-\hat{A})\,\psi\right] \times \psi^\dagger(x)\,S_{\bar{Q}}(x,y|A)\,\psi(y) \tag{86}$$

(unless stated otherwise, all expressions are written in Euclidean space), where $S_{\bar{Q}}(x,y|A)$ is the propagator of the static antiquark placed at the origin. To proceed, it is convenient to choose a particular version of the Fock–Schwinger gauge allowing us to express the vector potential in terms of the field tensor [66],

$$\mathbf{xA}(x_4,\mathbf{x})=0,\quad A_4(x_4,\mathbf{0})=0\,. \tag{87}$$

This particular gauge condition proves convenient, because the gluonic field vanishes at the trajectory of the static antiquark, and hence its Green's function takes a particularly simple form,

$$\begin{aligned}S_{\bar{Q}}(x,y|A)&=S_{\bar{Q}}(x,y)\\&=i\,\frac{1-\gamma_4}{2}\,\theta(x_4-y_4)\,\exp\left[-M(x_4-y_4)\right]\\&\quad+i\,\frac{1+\gamma_4}{2}\,\theta(y_4-x_4)\,\exp\left[-M(y_4-x_4)\right],\end{aligned} \tag{88}$$

where θ is a step-like function.

It is then easy to notice that Eqn (86) takes the form

$$S_{q\bar{Q}}(x,y)=\frac{1}{N_c}\int D\psi D\psi^\dagger \exp\left(-\int d^4x L_{\rm eff}(\psi,\psi^\dagger)\right) \times \psi^\dagger(x)\,S_{\bar{Q}}(x,y)\,\psi(y)\,, \tag{89}$$

that is, the antiquark is completely decoupled from the system and the dynamics of the light quark is defined by the effective Lagrangian $L_{\rm eff}(\psi,\psi^\dagger)$ such that

$$\begin{aligned}\int d^4x L_{\rm eff}(\psi,\psi^\dagger)&=\int d^4x\psi_\alpha^\dagger(x)(-i\hat{\partial}-im)\,\psi^\alpha(x)\\&+\int d^4x\psi_\alpha^\dagger(x)\,\gamma_\mu\psi^\beta(x)\langle\langle A_{\mu\beta}^{\ \alpha}\rangle\rangle\\&+\frac{1}{2}\int d^4x_1\,d^4x_2\psi_{\alpha_1}^\dagger(x_1)\,\gamma_{\mu_1}\psi^{\beta_1}(x_1)\,\psi_{\alpha_2}^\dagger(x_2)\,\gamma_{\mu_2}\psi^{\beta_2}(x_2)\\&\times\langle\langle A_{\mu_1\beta_1}^{\ \alpha_1}(x_1)A_{\mu_2\beta_2}^{\ \alpha_2}(x_2)\rangle\rangle+\ldots\,,\end{aligned} \tag{90}$$

where α and β are color indices in the fundamental representation, and the gluon field enters the form of irreducible correlators $\langle\langle A_{\mu_1\beta_1}^{\ \alpha_1}(x_1)\ldots A_{\mu_n\beta_n}^{\ \alpha_n}(x_n)\rangle\rangle$ of all orders, as was already mentioned in the Introduction. Retaining only the first nonvanishing (that is, Gaussian) correlator is an approximation (here, it is taken into account that $\langle\langle A_{\mu\beta}^{\ \alpha}\rangle\rangle=\langle A_{\mu\beta}^{\ \alpha}\rangle=0$). Discussions on the justification for this approximation can be found, e.g., in review paper [14]. It is also important to mention the results of lattice calculations [67] and their relation to the Casimir scaling in QCD traced in [68, 69].

Then, defining the interaction kernel of the two quark currents in terms of the bilocal correlator of the gluon fields in the vacuum,

$$\begin{aligned}\langle\langle A_{\mu\beta}^{\ \alpha}(x)\,A_{\nu\delta}^{\ \gamma}(y)\rangle\rangle&=\langle A_{\mu\beta}^{\ \alpha}(x)\,A_{\nu\delta}^{\ \gamma}(y)\rangle\\&\equiv 2(\lambda_a)_\beta^\alpha(\lambda_a)_\delta^\gamma K_{\mu\nu}(x,y)\,,\end{aligned} \tag{91}$$

using the Fierz identity $(\lambda_a)_\beta^\alpha(\lambda_a)_\delta^\gamma=1/2\delta_{\alpha\delta}\,\delta_{\gamma\beta}-(1/2N_c)\times\delta_{\alpha\beta}\,\delta_{\gamma\delta}$, and taking the limit of the infinite number of colors, we can write

$$\begin{aligned}L_{\rm eff}(\psi,\psi^\dagger)&=\psi_\alpha^\dagger(x)(-i\hat{\partial}-im)\,\psi^\alpha(x)\\&+\frac{1}{2}\int d^4y\,\psi_\alpha^\dagger(x)\,\gamma_\mu\psi^\beta(x)\,\psi_\beta^\dagger(y)\,\gamma_\nu\psi^\alpha(y)\,K_{\mu\nu}(x,y)\,,\end{aligned} \tag{92}$$

which implies the Schwinger–Dyson equation for the light quark in the form [60, 62, 63]

$$\begin{aligned}&(-i\hat{\partial}_x-im)\,S(x,y)-i\int d^4zM(x,z)\,S(z,y)=\delta^{(4)}(x-y)\,,\\&-iM(x,z)=K_{\mu\nu}(x,z)\,\gamma_\mu S(x,z)\,\gamma_\nu\,.\end{aligned} \tag{93}$$

Here, $S(x,y)=(1/N_c)\,\langle\psi^\beta(x)\,\psi_\beta^\dagger(y)\rangle$. It is instructive to note that although (93) looks like a single-particle equation, it nevertheless contains information about the heavy antiquark, because the kernel $K_{\mu\nu}$ is evaluated in gauge (87), which is closely related to the static antiquark placed at the origin.

Using the aforementioned property of gauge condition (87), we can express the vector potential of the gluon field in terms of the field tensor [66],

$$\begin{aligned}A_4^a(x_4,\mathbf{x})&=\int_0^1 x_iF_{i4}^a(x_4,\alpha\mathbf{x})\,d\alpha\,,\\A_i^a(x_4,\mathbf{x})&=\int_0^1 \alpha x_kF_{ki}^a(x_4,\alpha\mathbf{x})\,d\alpha\,,\quad i=1,2,3,\end{aligned} \tag{94}$$

and therefore the interaction kernel $K_{\mu\nu}$ can be expressed through the field correlator $\langle F_{\mu\nu}^a(x)F_{\lambda\rho}^b(y)\rangle$. Then, with the help of the vacuum background correlators method (see review [14]) and retaining only the confining part of the interaction, we can arrive at the kernel $K_{\mu\nu}(x,y)=$

$K_{\mu\nu}(x_4 - y_4, \mathbf{x}, \mathbf{y})$ (with $\tau = x_4 - y_4$) in the form (see [60, 61, 70] for a detailed derivation)

$$K_{44}(\tau, \mathbf{x}, \mathbf{y}) = (\mathbf{xy}) \int_0^1 \mathrm{d}\alpha \int_0^1 \mathrm{d}\beta D(\tau, |\alpha\mathbf{x} - \beta\mathbf{y}|)\,,$$
$$K_{i4}(\tau, \mathbf{x}, \mathbf{y}) = K_{4i}(\tau, \mathbf{x}, \mathbf{y}) = 0\,, \qquad (95)$$
$$K_{ik}(\tau, \mathbf{x}, \mathbf{y}) = \big((\mathbf{xy})\delta_{ik} - y_i x_k\big) \int_0^1 \alpha\,\mathrm{d}\alpha \int_0^1 \beta\,\mathrm{d}\beta D(\tau, |\alpha\mathbf{x} - \beta\mathbf{y}|)\,,$$

where the function $D(\tau, \lambda)$ decreases in all directions and describes the profile of the bilocal correlator of the nonperturbative gluon fields in the QCD vacuum (see review [14]).

Equation (93) is essentially nonlinear. It can, however, be linearized if the free Green's function is substituted, $S(x,z) \to S_0(x,z)$, into the mass operator $M(x,z)$. Such an approach, appropriate in the heavy-quark limit, was used in [59, 61] to derive the effective potentials and the spin-dependent corrections to it. The leading correction due to the proper dynamics of the string was found in [71]. But the above linearization is only possible if $mT_{\mathrm{g}} \gg 1$ [61], where m is the mass of the quark and T_{g} is the correlation length of the vacuum, which governs the decrease in the correlator D (see [72, 73] and the references therein for the extraction of the correlation length from the interquark potentials). In the opposite limit $mT_{\mathrm{g}} \ll 1$, such a linearization procedure is misleading and results in a divergent series [61], and nonlinear equation (93) therefore has to be studied in the full form in this limit. Inasmuch as the question discussed in this section is related to the spontaneous breaking of chiral symmetry, we must have a small quark mass, and it is therefore exactly the nonpotential regime with $mT_{\mathrm{g}} \ll 1$ that is adequate for the situation. Thus, we have to use a different simplification scheme for the equation. To begin, we disregard the spatial part of kernel (95), K_{ik}, which does not affect the qualitative result. We then take the Fourier transform of K_{44} in time,

$$K_{44}(\omega, \mathbf{x}, \mathbf{y}) \equiv K(\omega, \mathbf{x}, \mathbf{y}) = K(\mathbf{x}, \mathbf{y})$$
$$= \mathbf{xy} \int_0^1 \mathrm{d}\alpha \int_0^1 \mathrm{d}\beta \int_{-\infty}^{\infty} \mathrm{d}\tau\, D\big(\tau, |\alpha\mathbf{x} - \beta\mathbf{y}|\big)\,. \qquad (96)$$

To proceed, we note that the vacuum correlation length extracted from the lattice data is very small compared to the other scales of the problem ($T_{\mathrm{g}} \lesssim 0.1$ fm [72, 73]). It is therefore natural to take the so-called string limit $T_{\mathrm{g}} \to 0$, which, given the normalization condition,

$$\sigma = 2 \int_0^{\infty} \mathrm{d}\nu \int_0^{\infty} \mathrm{d}\lambda\, D(\nu, \lambda)\,, \qquad (97)$$

where the parameter σ defines the tension of the QCD string [14], yields a δ-function-like profile for the correlator,

$$D(\tau, \lambda) = 2\sigma\delta(\tau)\,\delta(\lambda)\,, \qquad (98)$$

whence

$$K(\mathbf{x}, \mathbf{y}) = 2\sigma(\mathbf{xy}) \int_0^1 \mathrm{d}\alpha \int_0^1 \mathrm{d}\beta\, \delta\big(|\alpha\mathbf{x} - \beta\mathbf{y}|\big)\,. \qquad (99)$$

The fact that kernel (99) does not vanish only for collinear vectors $\mathbf{x}$ and $\mathbf{y}$ is a consequence of the infinitely thin (in the limit $T_{\mathrm{g}} \to 0$) string connecting the quark and the antiquark. Then the integral in (99) can be taken exactly to yield

$$K(\mathbf{x}, \mathbf{y}) = 2\sigma \min\big(|\mathbf{x}|, |\mathbf{y}|\big)$$
$$= \begin{cases} \sigma\big(|\mathbf{x}| + |\mathbf{y}| - |\mathbf{x} - \mathbf{y}|\big)\,, & \mathbf{x} \parallel \mathbf{y}\,, \\ 0\,, & \mathbf{x} \nparallel \mathbf{y}\,. \end{cases} \qquad (100)$$

The obtained expression can be viewed as a three-dimensional generalization of the one-dimensional kernel derived in [20] for the 't Hooft model. We note that the condition of collinearity for the vectors $\mathbf{x}$ and $\mathbf{y}$ is trivial for only one spatial dimension; however, for kernel (100) it leads to technical complications not important for the mechanisms of spontaneous chiral symmetry breaking. Therefore, it is natural to relax this condition and, for any $\mathbf{x}$ and $\mathbf{y}$, to consider the interaction kernel in the form

$$K(\mathbf{x}, \mathbf{y}) = \sigma\big(|\mathbf{x}| + |\mathbf{y}| - |\mathbf{x} - \mathbf{y}|\big)\,. \qquad (101)$$

This kernel has a number of attractive features, such as

• it allows one to pass more trivially from Euclidean space to Minkowski space; from now on, only Minkowski space is considered;

• it has a simple physical interpretation: the part $-\sigma|\mathbf{x} - \mathbf{y}|$ describes the self-interaction of the light quark, while the term $\sigma(|\mathbf{x}| + |\mathbf{y}|)$ is responsible for the interaction of the quark with the static antiquark. The fact that both interactions are encoded in the same kernel is a consequence of gauge condition (87), which results in the static antiquark decoupling from the system. Then, because the gauge condition violates translation invariance, kernel (101) does not demonstrate such an invariance either;

• it allows a natural generalization to an arbitrary profile of the interquark interaction potential $V(r)$, such that the generic form of the kernel is

$$K(\mathbf{x}, \mathbf{y}) = V(|\mathbf{x}|) + V(|\mathbf{y}|) - V(|\mathbf{x} - \mathbf{y}|)\,; \qquad (102)$$

• it establishes a natural relation between the vacuum background correlators method and the GNJL model, because from now on any equation can be derived with the help of either of the two approaches.

Although the above considerations cannot be treated as a true derivation of the GNJL model from QCD, it nevertheless allows establishing a close relation between the fundamental theory and this model. In the literature, one can find a similar derivation of the Hamiltonian in the form of Eqn (1) in the Gaussian approximation for the QCD vacuum (see [74]), as well as attempts at a more rigorous derivation of the classic NJL model from QCD (see, in particular, [36, 37]).

We are now in a position to return to the equation for the heavy–light quarkonium. In particular, Schwinger–Dyson equation (93) for the light quark can be written in the form

$$\left(-\mathrm{i}\gamma_0 \frac{\partial}{\partial t} + \mathrm{i}\boldsymbol{\gamma} \frac{\partial}{\partial \mathbf{x}} - m\right) S(t, \mathbf{x}, \mathbf{y})$$
$$- \int \mathrm{d}^3 z M(\mathbf{x}, \mathbf{z})\, S(t, \mathbf{z}, \mathbf{y}) = \delta(t)\, \delta^{(3)}(\mathbf{x} - \mathbf{y})\,, \qquad (103)$$

where

$$M(\mathbf{x}, \mathbf{z}) = -\frac{\mathrm{i}}{2}\, K(\mathbf{x}, \mathbf{z})\, \gamma_0 \Lambda(\mathbf{x}, \mathbf{z})\,,$$
$$\Lambda(\mathbf{x}, \mathbf{z}) = 2\mathrm{i} \int \frac{\mathrm{d}\omega}{2\pi}\, S(\omega, \mathbf{x}, \mathbf{z})\, \gamma_0\,. \qquad (104)$$

The Lorentz nature of the interaction described by the kernel K depends on the matrix structure of the mass operator $M(\mathbf{x},\mathbf{y})$. Thus, if $M(\mathbf{x},\mathbf{y})$ acquires a contribution proportional to the unit matrix, it gives rise to an interaction added to the mass, that is, to scalar confinement. For a detailed study of this problem, we use the natural separation of kernel (101) into the local and nonlocal parts. As was explained above, the local part of the kernel is responsible for the light quark self-interaction and therefore defines the 'dressing' of the quark. Indeed, it is easy to see that omitting the nonlocal contribution $\sigma(|\mathbf{x}|+|\mathbf{y}|)$, we can proceed from Eqn (93) to the Dyson equation

$$\big(\gamma_0 p_0 - \boldsymbol{\gamma}\,\mathbf{p} - m - \Sigma(\mathbf{p})\big)\, S(p_0,\mathbf{p}) = 1\,, \tag{105}$$

where the mass operator for the light quark $\Sigma(\mathbf{p})$ takes the form

$$\Sigma(\mathbf{p}) = -\mathrm{i}\int \frac{\mathrm{d}^4 k}{(2\pi)^4}\, V(\mathbf{p}-\mathbf{k})\,\gamma_0 S(k_0,\mathbf{k})\,\gamma_0\,, \tag{106}$$

and, due to the instantaneous nature of the interaction, it does not depend on the energy. It is easy to verify that expression (106) for the mass operator reproduces Eqn (27), which was derived above by summing the Dyson series for the dressed-quark propagator (see Fig. 2).

Once the Green's function $S(p_0,\mathbf{p})$ is determined from Eqn (105), its substitution in (106) results in a self-consistency condition, which is nothing more than the mass-gap equation (30) in the GNJL model [21–29], which can be conveniently written as Eqn (14) for the chiral angle φ_p.

For the function $\Lambda(\mathbf{p},\mathbf{q})$ parameterized through the chiral angle, which is the double Fourier transform of $\Lambda(\mathbf{x},\mathbf{y})$ introduced in Eqn (104), it is straightforward to find

$$\Lambda(\mathbf{p},\mathbf{q}) = 2\mathrm{i}\int \frac{\mathrm{d}\omega}{2\pi}\, S(\omega,\mathbf{p},\mathbf{q})\,\gamma_0 = (2\pi)^3 \delta^{(3)}(\mathbf{p}-\mathbf{q})\, U_p\,, \tag{107}$$

where

$$U_p = \beta\sin\varphi_p + \boldsymbol{\alpha}\hat{\mathbf{p}}\cos\varphi_p\,,\quad \beta=\gamma_0\,,\quad \boldsymbol{\alpha}=\gamma_0\boldsymbol{\gamma}\,. \tag{108}$$

We revisit Eqn (103) and rewrite it in the form of the bound-state equation for the wave function $\tilde{\Psi}(\mathbf{x})$,

$$(\boldsymbol{\alpha}\hat{\mathbf{p}} + \beta m)\,\tilde{\Psi}(\mathbf{x}) + \beta\int \mathrm{d}^3 z M(\mathbf{x},\mathbf{z})\,\tilde{\Psi}(\mathbf{z}) = E\tilde{\Psi}(\mathbf{x})\,, \tag{109}$$

where both local and nonlocal parts of the kernel are now taken into account. Then, passing to the momentum space and using the mass-gap equation in the form

$$E_p U_p = \boldsymbol{\alpha}\mathbf{p} + \beta m + \frac{1}{2}\int \frac{\mathrm{d}^3 k}{(2\pi)^3}\, V(\mathbf{p}-\mathbf{k})\, U_k\,, \tag{110}$$

we can write Eqn (109) as

$$E_p U_p \tilde{\Psi}(\mathbf{p}) + \frac{1}{2}\int \frac{\mathrm{d}^3 k}{(2\pi)^3}\, V(\mathbf{p}-\mathbf{k})(U_p + U_k)\,\tilde{\Psi}(\mathbf{k}) = E\tilde{\Psi}(\mathbf{p})\,. \tag{111}$$

Equation (111) allows an exact Foldy–Wouthuysen transformation [75],[2]

[2] This possibility is closely related to the instantaneous nature of the interaction and to the presence of an infinitely heavy particle in the system [16].

$$\begin{gathered}\tilde{\Psi}(\mathbf{p}) = T_p \Psi(\mathbf{p})\,,\quad \Psi(\mathbf{p}) = \begin{pmatrix}\psi(\mathbf{p})\\ 0\end{pmatrix},\\ T_p = \exp\left[-\frac{1}{2}\,\boldsymbol{\gamma}\,\hat{\mathbf{p}}\left(\frac{\pi}{2}-\varphi_p\right)\right],\end{gathered} \tag{112}$$

which brings it to a Schrödinger-like equation for the two-component spinor for the light quark $\psi(\mathbf{p})$,

$$\begin{aligned}E_p\psi(\mathbf{p}) &+ \int \frac{\mathrm{d}^3 k}{(2\pi)^3}\, V(\mathbf{p}-\mathbf{k})\\ &\times\big(C_p C_k + (\boldsymbol{\sigma}\hat{\mathbf{p}})(\boldsymbol{\sigma}\hat{\mathbf{k}})\, S_p S_k\big)\,\psi(\mathbf{k}) = E\psi(\mathbf{p})\,,\end{aligned} \tag{113}$$

where C_p and S_p are defined in (40).

Before we study the properties of Eqn (113) in detail, we derive it directly in the framework of the GNJL model. First of all, we note that the bound-state equation for quark–antiquark system (37) is symmetric under the change

$$\big\{M_n, \varphi_n^{\pm}(\mathbf{p})\big\} \leftrightarrow \big\{-M_n, \varphi_n^{\mp}(\mathbf{p})\big\}\,. \tag{114}$$

As was explained in Section 3.2, the two components of the wave function, $\varphi_n^+(p)$ and $\varphi_n^-(p)$, describe the motion of the quark–antiquark pair forward and backward in time in the meson and, what is more, because of the instantaneous form of interaction kernel (2), the quark and the antiquark can only move back and forth in time in unison. Therefore, because the static antiquark can never move back in time, the other quark is forced to do the same. It can thus be expected that in the limit of the static antiquark, system (45) splits into two decoupled equations.

Indeed, Eqn (33) is generalized to the heavy–light system as

$$\begin{aligned}\chi(\mathbf{p};M) = -\mathrm{i}\int \frac{\mathrm{d}^4 k}{(2\pi)^4}\, V(\mathbf{p}-\mathbf{k})\,\gamma_0 S_{\mathrm{q}}\left(\mathbf{k},k_0+\frac{M}{2}\right)\\ \times\chi(\mathbf{k};M)\, S_{\bar{\mathrm{Q}}}\left(\mathbf{k},k_0-\frac{M}{2}\right)\gamma_0\,,\end{aligned} \tag{115}$$

where, similarly to Eqn (28),

$$S_{\mathrm{q}}(\mathbf{p},p_0) = \frac{\Lambda^+(\mathbf{p})\,\gamma_0}{p_0 - E_p + \mathrm{i}0} + \frac{\Lambda^-(\mathbf{p})\,\gamma_0}{p_0 + E_p - \mathrm{i}0}\,, \tag{116}$$

$$\Lambda^{\pm}(\mathbf{p}) = T_p P_{\pm} T_p^{\dagger}\,,\quad P_{\pm} = \frac{1\pm\gamma_0}{2}\,, \tag{117}$$

while the chiral angle for the static antiquark is simply $\varphi_{\bar{\mathrm{Q}}}(p) \equiv \pi/2$, and hence the positive- and negative-energy projectors take a simpler form, as does the Green's function of the antiquark,

$$S_{\bar{\mathrm{Q}}}(\mathbf{p},p_0) = \frac{P_+\gamma_0}{p_0 - m_{\bar{\mathrm{Q}}} + \mathrm{i}0} + \frac{P_-\gamma_0}{p_0 + m_{\bar{\mathrm{Q}}} - \mathrm{i}0}\,. \tag{118}$$

Similarly to the generic case [see Eqn (44)], it proves convenient to define the matrix wave function

$$\tilde{\phi}(\mathbf{p}) = \int \frac{\mathrm{d}p_0}{2\pi}\, S_{\mathbf{q}}\left(\mathbf{p},p_0+\frac{M}{2}\right)\chi(\mathbf{p};M)\, S_{\bar{\mathrm{Q}}}\left(\mathbf{p},p_0-\frac{M}{2}\right), \tag{119}$$

which is subject to the Foldy–Wouthuysen transformation by the operator T_p [see definition (112)] from the left (for the light quark) and by the operator $T_p(\varphi_p \equiv \pi/2) = \hat{1}$ from the right (for the static antiquark),

$$\tilde{\phi}(\mathbf{p}) = T_p \phi(\mathbf{p})\,\hat{1}\,. \tag{120}$$

It is then easy to arrive at the equation

$$(E - E_p)\,\phi(\mathbf{p}) = P_+ \left[\int \frac{d^3 k}{(2\pi)^3}\, V(\mathbf{p}-\mathbf{k})\, T_p^\dagger T_k \phi(\mathbf{k}) \right] P_-\,, \tag{121}$$

where $E = M - m_{\bar{Q}}$ is the excess of energy over the mass of the static antiquark. The form of the solution of Eqn (121) follows from the projectors in the right-hand side,

$$\phi(\mathbf{p}) = \begin{pmatrix} 0 & \psi(\mathbf{p}) \\ 0 & 0 \end{pmatrix} = \begin{pmatrix} \psi(\mathbf{p}) \\ 0 \end{pmatrix} \otimes (0\ 1) = \Psi(\mathbf{p}) \otimes \Psi_{\bar{Q}}^{\mathrm{T}}(\mathbf{p})\,, \tag{122}$$

where the right-hand side is written in the form of the tensor product of the components describing the light [see Eqn (112)] and the heavy degrees of freedom. Substituting the explicit form of the operators T_p and T_k in (121), it is easy to reproduce Eqn (113).

Due to symmetry (114) of system (45), the solution for the meson with the energy $M_n = -m_{\bar{Q}} - E_n$ can be obtained with the help of the same (inverse) Foldy–Wouthuysen transformation (120), now applied to the wave function $(0, \psi(\mathbf{p}))^{\mathrm{T}}$. As a result, we can reproduce Eqn (109) with the propagator given by [75],

$$S(\omega, \mathbf{p}, \mathbf{k}) = \sum_{E_n > 0} \frac{\tilde{\Psi}_n(\mathbf{p}) \tilde{\Psi}_n^\dagger(\mathbf{k})\, \gamma_0}{\omega - E_n + \mathrm{i}0} + \sum_{E_n < 0} \frac{\tilde{\Psi}_n(\mathbf{p})\, \tilde{\Psi}_n^\dagger(\mathbf{k})\, \gamma_0}{\omega + E_n - \mathrm{i}0}\,, \tag{123}$$

while for the quantity $\Lambda(\mathbf{p}, \mathbf{k})$, result (107) is reproduced with

$$U_p = T_p \gamma_0 T_p^\dagger\,. \tag{124}$$

Equations (103) and (113) allow us to answer the question on the Lorentz nature of the confining interaction in the heavy–light quarkonium. For low-lying states with a small relative momentum between the quarks, the chiral angle φ_p takes values close to $\pi/2$ (see Fig. 1). Then, in the limit $\varphi_p = \pi/2$, it is easy to find that $C_p = 1$, $S_p = 0$, and it is then straightforward to pass to the coordinate space in Eqn (113), and the interaction reduces to the linear potential σr. If, in addition, the kinetic term E_p is substituted by the energy of the free particle,[3] the resulting equation reproduces the Salpeter equation

$$\left(\sqrt{\mathbf{p}^2 + m^2} + \sigma r \right) \psi = E \psi\,, \tag{125}$$

which is commonly used in the literature on hadronic spectroscopy (see, e.g., [76, 77]).

On the other hand, for $\varphi_p = \pi/2$, we have $U_p = \gamma_0$, and therefore

$$\Lambda(\mathbf{x}, \mathbf{y}) = \gamma_0 \delta^{(3)}(\mathbf{x} - \mathbf{y})\,, \quad M(\mathbf{x}, \mathbf{y}) = \sigma |\mathbf{x}|\, \delta^{(3)}(\mathbf{x} - \mathbf{y})\,, \tag{126}$$

[3] This procedure is definitely ill-defined for the chiral pion; however, for the other mesonic states, it provides a rough but rather adequate approximation.

whence we see that the entire potential $\sigma|\mathbf{x}|$ is added to the mass in Eqn (103), that is, the interquark interaction is purely scalar. It is important to note that this scalar has essentially dynamical origins apparently entirely due to the chiral angle deviation from the trivial solution, which, in turn, is closely related to the effect of chiral symmetry breaking in a vacuum.

In the opposite limit of large interquark momenta, when the chiral angle decreases and tends to zero, the contribution of the scalar interaction also decreases, but, on the contrary, the contribution of the (spatial) vectorial interaction increases. This regime is realized for highly excited states in the spectrum of hadrons (see a detailed discussion of this problem in Section 5). It has to be noted that the matrix $\Lambda(\mathbf{p}, \mathbf{k})$ does not contain contributions proportional to the unit matrix, which could have brought about the temporal component of the increasing-with-distance vectorial interaction and which would therefore be potentially dangerous from the standpoint of the Klein paradox.

In short, we used the heavy–light quark–antiquark system to demonstrate, at the microscopic level, the emergence of the effective scalar interquark interaction as a result of the phenomenon of spontaneous chiral symmetry breaking in a vacuum. Moreover, we traced the connection between the GNJL model and QCD in the Gaussian approximation for gluon fields in a vacuum.

5. Effective chiral symmetry restoration in the spectrum of hadrons

5.1 Introductory comments

In Sections 2–4, the GNJL model was used to address the phenomenon of spontaneous chiral symmetry breaking in a vacuum microscopically. In addition, the properties of the chiral pion — the lowest state in the spectrum of hadrons, which also plays the role of a pseudo-Goldstone boson — were described in detail. Meanwhile, there are good reasons to expect that the effects of spontaneously broken chiral symmetry are not manifested in the spectrum of excited hadrons, and it is therefore relevant to discuss its effective restoration and how it occurs (see review [54] and the references therein). We emphasize that the discussion in this section concerns the way chiral symmetry is realized in the spectrum of excited hadrons; in particular, it is demonstrated that the properties of highly excited hadrons are only weakly sensitive to the phenomenon of spontaneous chiral symmetry breaking in a vacuum. This entails various observable consequences, which are also discussed below.

In [75, 78–83], this phenomenon was described in the framework of various approaches to QCD. Regardless of the particular model used, such an effective chiral symmetry restoration implies the emergence of multiplets of hadronic states approximately degenerate in mass. An important comment is in order here. It is well known that the mass spectrum of quark–antiquark mesons bound by a linear potential shows a Regge behavior, that is, $M_{n,l}^2 \propto n$ and $M_{n,l}^2 \propto l$ for $n, l \gg 1$. Here, n and l are the radial quantum number and the angular momentum. It is easy to see that states with the opposite parity, which form approximately degenerate doublets, have angular momenta different by one unit (for example, the scalar $^3P_0$ and the pseudo-scalar $^1S_0$). Therefore, for a given angular momentum l_0, the splitting in such a pair is

$$\Delta M^{+-}_{n,l_0} \equiv M^{+}_{n,l_0+1} - M^{-}_{n,l_0} \sim \frac{1}{M^{+}_{n,l_0+1} + M^{-}_{n,l_0}} \sim \frac{1}{\sqrt{n}}\,, \quad (127)$$

which decreases as the radial quantum number increases. Clearly, such a decrease does not imply effective chiral symmetry restoration. Indeed, exactly the same dependence takes place for the splitting between same-parity neighbors,

$$\Delta M^{\pm\pm}_{n,l_0} \equiv M^{\pm}_{n,l_0+1} - M^{\pm}_{n,l_0} \sim \frac{1}{M^{\pm}_{n,l_0+1} + M^{\pm}_{n,l_0}} \sim \frac{1}{\sqrt{n}}\,, \quad (128)$$

which has nothing to do with chiral symmetry. Therefore, it is necessary to define the quantity that would allow deciding whether the effective restoration of chiral symmetry in the spectrum occurs. For such a quantity, we can choose the splitting between the masses squared, $\Delta(M^{+-})^2 = (M^+)^2 - (M^-)^2$, [75] [4] or, equivalently, the ratio of the splittings $\Delta M^{+-}/\Delta M^{\pm\pm}$ within the same chiral multiplet [84].

Thus, it would be natural to use the microscopic approach to chiral symmetry breaking provided by the GNJL model in order to study the influence of chiral symmetry breaking on the spectrum of excited hadrons.

5.2 Quantum fluctuations and the semiclassical regime in the spectrum of excited hadrons

The phenomenon of effective restoration of chiral symmetry in the spectrum of excited hadrons has a simple qualitative explanation. Inasmuch as spontaneous breaking of chiral symmetry is a consequence of quantum fluctuations (loops), it must be a quantum effect itself. The parameter characterizing the role played by such fluctuations is provided by the ratio $\hbar/\mathcal{S}$, where $\mathcal{S}$ is the classical action responsible for the internal degrees of freedom in a hadron. For large values of the quantum numbers, that is, in the semiclassical region of the spectrum, we have $\mathcal{S} \gg \hbar$, and therefore the effect of spontaneous chiral symmetry breaking cannot affect the properties of highly excited hadrons [85].

Below, we exemplify this qualitative picture with the help of the GNJL mode. As before, we take the large-N_c limit, which allows us to consider only planar (ladder and rainbow) diagrams; in addition, for illustrative purposes, we restrict ourselves to the simplest structure of the confining potential, $\gamma_0 \times \gamma_0$, [see Eqn (2)].

We consider Dyson equation (30) for the mass operator. Similarly to many nonlinear equations, this equation has several solutions. One of them is perturbative, and it is given by the series

$$\Sigma = \int d^4k\; V\gamma_0 S_0 \gamma_0 + \int d^4k\, d^4q\; V^2 \gamma_0 S_0 \gamma_0 S_0 \gamma_0 S_0 \gamma_0 + \ldots\,, \quad (129)$$

which rapidly converges in the weak-interaction limit. It is easy to demonstrate that this solution is nothing but a series in the powers of the Planck constant $\hbar$. For this, we restore it explicitly in formula (30).

[4] For generic power-law potential (3), the power of the masses to be considered is $(\alpha+1)/\alpha$.

The confining potential is defined by the averaged Wilson loop

$$\langle W(C) \rangle = \exp\left(-\frac{\sigma A}{\hbar c}\right), \quad (130)$$

where σ is the string tension and A is the area of the minimal surface in Euclidean space bounded by the contour C. For convenience, the speed of light c is also shown explicitly, but is to be omitted later when appropriate. Then, for a rectangular loop,

$$\frac{\sigma A}{\hbar c} = \frac{\sigma R(cT)}{\hbar c} = \frac{1}{\hbar}\int_0^T \sigma R\, dt = \frac{1}{\hbar}\int_0^T V(R)\, dt\,. \quad (131)$$

From Eqn (131), it is easy to find the linear confinement $V(r) = \sigma r$ as the interquark potential, which is assumed to be a classical quantity surviving in the formal classical limit $\hbar \to 0$. For its Fourier transform, we then find

$$V(\mathbf{p}) = \int d^3x \exp\left(\frac{i\mathbf{p}\mathbf{x}}{\hbar}\right)\sigma|\mathbf{x}| = -\frac{8\pi\sigma\hbar^4}{p^4} = \hbar^4 \tilde{V}(\mathbf{p})\,, \quad (132)$$

where the quantity $\tilde{V}(\mathbf{p})$ does not contain $\hbar$. As a result, it is easy to arrive at

$$i\Sigma(\mathbf{p}) = \hbar \int \frac{d^4k}{(2\pi)^4}\,\tilde{V}(\mathbf{p}-\mathbf{k})\,\gamma_0\,\frac{1}{S_0^{-1}(k_0,\mathbf{k}) - \Sigma(\mathbf{k})}\,\gamma_0\,, \quad (133)$$

where the factor $\hbar^4$ from the potential in the numerator cancels the factor $\hbar^4$ from the differential $d^4k/(2\pi\hbar)^4$ in the denominator. The remaining $\hbar$ is easily restored to provide the correct dimension of the right-hand side. Therefore, the perturbative expansion in powers of potential (129) is a loop expansion, and each power of the potential (each loop) brings $\hbar$.

We next consider mass-gap equation (14) with the Planck constant $\hbar$ and the speed of light c restored explicitly:

$$pc\sin\varphi_p - mc^2\cos\varphi_p = \frac{\hbar}{2}\int \frac{d^3k}{(2\pi)^3}\,\tilde{V}(\mathbf{p}-\mathbf{k}) \times \left(\cos\varphi_k \sin\varphi_p - \hat{\mathbf{p}}\hat{\mathbf{k}}\,\sin\varphi_k\cos\varphi_p\right). \quad (134)$$

We study the limit $m = 0$ first. It is easy to see that in the formal classical limit $\hbar \to 0$, the right-hand side of Eqn (134) vanishes and the only solution of this equation is the trivial chirally symmetric solution $\varphi_p = 0$. This result is quite natural because, for $m = 0$, the chiral angle parameterizes the loop contribution, which is a purely quantum effect and which must therefore vanish in the classical limit. Any attempt to find a solution of Eqn (134) in the form of a series in powers of $\hbar$, $\varphi_p = \hbar f_1(p) + \hbar^2 f_2(p) + \ldots$, has to fail, because all coefficients in such a series vanish. This should not come as a surprise either, for it has a simple qualitative explanation. Indeed, the full form of the given expansion of the chiral angle in powers of $\hbar$ should look like

$$\varphi_p = \frac{\hbar}{\mathcal{S}} f_1\left(\frac{p}{\mu c}\right) + \frac{\hbar^2}{\mathcal{S}^2} f_2\left(\frac{p}{\mu c}\right) + \ldots\,, \quad (135)$$

where the Planck constant enters divided by the quantity $\mathcal{S}$, which has the dimension of action, while the momentum is measured in units of some mass parameter μ. It is easy to verify that the only two dimensional parameters at hand, σ and c, are not sufficient to build the quantity $\mathcal{S}$, and this fact alone automatically invalidates expansion (135).

To gain an insight into the behavior of the chiral angle in the classical limit, we proceed to the dimensionless mass-gap equation obtained from (134) by the substitution $\mathbf{p} = \mu c \boldsymbol{\xi}$ and $\mathbf{k} = \mu c \boldsymbol{\eta}$, such that all dimensional parameters in the equation produce a single mass scale $\mu = \sqrt{\sigma \hbar c}/c^2$. It easy to see that the scale μ depends on the Planck constant. Then the small-momentum expansion of the chiral angle has the form

$$\varphi_p \underset{p\to 0}{\approx} \frac{\pi}{2} - \mathrm{const}\,\frac{pc}{\mu c^2} + \ldots = \frac{\pi}{2} - \mathrm{const}\,\frac{pc}{\sqrt{\sigma\hbar c}} + \ldots\,,$$

and therefore, in the formal limit $\hbar \to 0$, the chiral angle becomes steeper at the origin, thus approaching the chirally symmetric solution $\varphi_p = 0$. In other words, we witness a collapse of the chiral angle, similar to the one that happens to the quantum mechanical wave function in the classical limit. Indeed, the chiral angle can be viewed as the radial wave function of quark–antiquark pairs in a vacuum [see, e.g., formula (19)]. Furthermore, the chiral angle defines the wave function of the chiral pion. Thus, the chiral angle — the solution of the mass-gap equation — depends on the Planck constant essentially nonperturbatively.

Beyond the chiral limit, if the quark mass is introduced as a perturbation, the chiral angle can be represented as a series in powers of the small dimensionless parameter $mc^2/\sqrt{\sigma\hbar c}$,

$$\varphi_p = \sum_{n=0}^{\infty} \left(\frac{mc^2}{\sqrt{\sigma\hbar c}}\right)^n f_n\left(\frac{pc}{\sqrt{\sigma\hbar c}}\right). \tag{136}$$

The leading term $f_0(p)$ is plotted in Fig. 1.

On the other hand, as was mentioned above, beyond the chiral limit, the quark mass m, by furnishing an additional dimensional parameter, allows building both the classical dimension of the action, $\mathcal{S} \sim m^2c^3/\sigma$, and the classical dimension of the momentum, mc. Then expansion (135) becomes possible and takes the form

$$\varphi_p = \sum_{n=0}^{\infty} \left(\frac{\sigma\hbar c}{(mc^2)^2}\right)^n \tilde{f}_n\left(\frac{p}{mc}\right), \tag{137}$$

and hence the dimensionless expansion parameter is given by $\sigma\hbar c/(mc^2)^2$. The leading term in series (137) is known analytically and is given by the free chiral angle $\tilde{f}_0 = \arctan(mc/p)$. In other words, perturbative solution (137) is given by expansion (129).

Both expansions (136) and (137) reproduce the same solution for the chiral angle. However, expansion (136) converges fast near the chiral limit with $m = 0$ and beyond the classical limit with $\hbar \neq 0$ (expansion (137) blows up in this limit). On the contrary, for $m \gg \sqrt{\sigma\hbar c}/c^2$, expansion (137) converges much better than expansion (136). Meanwhile, there is no one-to-one correspondence between the functions $\{f_n\}$ and $\{\tilde{f}_n\}$, and each function from one set is given by an infinite series in terms of the functions from the other set. For example, for asymptotically large momenta, the function f_0, depicted in Fig. 1, tends to zero as $1/p^5$ [see Eqn (25)], while the asymptotic behavior of $\tilde{f}_0$ is much slower, $1/p$.

As a final remark, we note that expansions (136) and (137) explicitly specify two dynamical regimes of the system depending on the value of the parameter $m/\sqrt{\sigma}$. Spontaneous chiral symmetry breaking occurs in the limit $m \ll \sqrt{\sigma}$ (regime (136)), while in the opposite limit $m \gg \sqrt{\sigma}$, we are dealing with 'heavy-quark' physics (regime (137)).

5.3 Effective chiral symmetry restoration in the spectrum of excited mesons

As was mentioned in Section 5.1, the spectrum of highly excited hadrons is expected to show the phenomenon of an effective restoration of chiral symmetry. In Section 5.2, general qualitative arguments were given in favor of such a restoration in the GNJL model. Below, we study this phenomenon quantitatively [75].

We start from Schrödinger equation (113) describing the mass spectrum of heavy–light quarkonia. Multiplying this equation by $(\boldsymbol{\sigma}\mathbf{p})$ from the left, we can rewrite the result in the form of the bound-state equation for the wave function

$$\psi'(\mathbf{p}) = \boldsymbol{\sigma}\hat{\mathbf{p}}\,\psi(\mathbf{p})\,, \tag{138}$$

which, by construction, has the opposite parity compared with $\psi(\mathbf{p})$. The resulting equation

$$E_p\psi'(\mathbf{p}) + \int \frac{d^3k}{(2\pi)^3}\, V(\mathbf{p}-\mathbf{k})\left[S_pS_k + (\boldsymbol{\sigma}\hat{\mathbf{p}})\,(\boldsymbol{\sigma}\hat{\mathbf{k}})\,C_pC_k\right] \times \psi'(\mathbf{k}) = E\psi'(\mathbf{p}) \tag{139}$$

differs from Eqn (113) by the permutation of the quantities C_p and S_p defined in (40). It is then easy to see that in the limit of large relative momenta, $\varphi_p \underset{p\to\infty}{\longrightarrow} 0$ (see Fig. 1), and hence $C_p = S_p = 1/\sqrt{2}$ and Eqns (113) and (139) coincide, taking the form

$$E_p\psi^{(\prime)}(\mathbf{p}) + \frac{1}{2}\int \frac{d^3k}{(2\pi)^3}\, V(\mathbf{p}-\mathbf{k})\left[1 + (\boldsymbol{\sigma}\hat{\mathbf{p}})(\boldsymbol{\sigma}\hat{\mathbf{k}})\right]\psi^{(\prime)}(\mathbf{k}) = E\psi^{(\prime)}(\mathbf{p})\,. \tag{140}$$

Therefore, the opposite-parity states $\psi(\mathbf{p})$ and $(\boldsymbol{\sigma}\hat{\mathbf{p}})\,\psi(\mathbf{p})$ become degenerate. We note that the Fourier transform of the potential in Eqns (113) and (139) picks up the region $\mathbf{p} \approx \mathbf{k}$, and therefore, approximately, we can speak of the effective restoration of chiral symmetry if $C_p^2 \approx S_p^2$. It is then easy to find that in the chiral limit,

$$C_p^2 - S_p^2 = \sin\varphi_p = \pm\mathcal{N}_\pi^{-1}\varphi_\pi^{\pm}(p)\,, \tag{141}$$

where $\varphi_\pi^{\pm}(p)$ are the components of the wave function of the chiral pion [see Eqn (55)]. This relation emphasizes the connection between the parity degeneracy observed in the spectrum of highly excited mesons and chiral symmetry. In Fig. 4, we can see the dependences of C_p^2 and S_p^2 on the momentum for potentials of the form $V(r) = K_0^{\alpha+1}r^\alpha$ with different values of the exponent α. It is easy to see from the plot that the above functions indeed reach the asymptotic value 1/2 fast.

As was mentioned above many times, qualitative predictions of the model do not depend on the exponent α. Moreover, quantitative predictions also demonstrate only a very weak dependence on α (see Fig. 4). Thus, for a detailed quantitative study of the problem of chiral symmetry restoration in the spectrum of highly excited mesons, it is sufficient to choose the exponent α that provides the simplest form of the equations, that is, $\alpha = 2$. Then

$$V(\mathbf{p}-\mathbf{k}) = -K_0^3\Delta_k\delta^{(3)}(\mathbf{p}-\mathbf{k})\,, \tag{142}$$

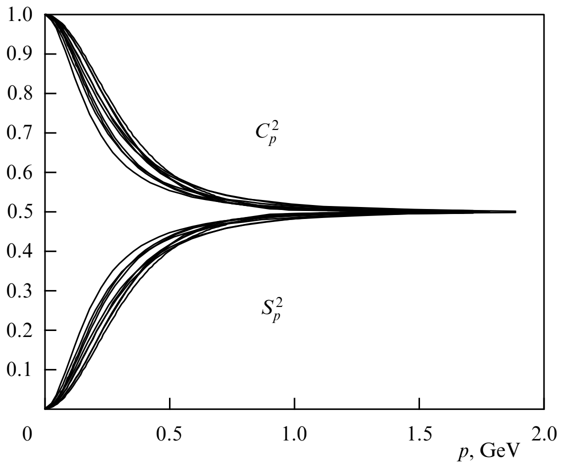

Figure 4. Momentum dependence of the coefficients C_p^2 and S_p^2 for the potential $V(r) = K_0^{\alpha+1} r^\alpha$ with $\alpha = 0.3$, 0.5, 0.7, 0.9, 1.0, 1.1, 1.3, 1.7, and 2.0. For each potential, the parameter K_0 is tuned to provide the same value of the chiral condensate, equal to $-(250\ \text{MeV})^3$.

and the mass-gap equation reduces to second-order differential equation (16). Chiral condensate (24) equals $-(0.51 K_0)^3$ and takes the standard value $-(250\ \text{MeV})^3$ for

$$K_0 = 490\ \text{MeV}\,. \tag{143}$$

It has to be noted that the most appropriate basis to deal with the spectrum of highly excited mesons and, in particular, to study the prevalence of chiral symmetry restoration is the chiral basis [55]. For example, in [86], this basis was successfully used for numerical studies of the mass spectrum of excited mesons in the GNJL model. Nevertheless, for better correspondence between the calculations done in the framework of the GNJL model and with the Salpeter equation, we adhere to the standard basis $\{J, L, S\}$. Then the wave function of the light quark $\psi(\mathbf{p})$ is decomposed in the basis of spherical spinors

$$\Omega_{jlm}(\hat{\mathbf{p}}) = \sum_{\mu_1 \mu_2} C^{jm}_{l\mu_1 (1/2)\mu_2} Y_{l\mu_1}(\hat{\mathbf{p}})\, \chi_{\mu_2} \tag{144}$$

as

$$\psi(\mathbf{p}) = \Omega_{jlm}(\hat{\mathbf{p}})\, \frac{u(p)}{p}\,, \tag{145}$$

where $u(p)$ is the radial wave function in the momentum representation, for which the following equation can be derived from (113):

$$u'' = (E_p - E)\, u + K_0^3 \left[\frac{\varphi_p'^2}{4} + \frac{\kappa}{p^2} (\kappa + \sin\varphi_p) \right] u\,, \tag{146}$$

and where the spin–orbit interaction for the central potential is introduced in the standard way,

$$\kappa = \begin{cases} l\,, & \text{for} \quad j = l - \dfrac{1}{2} \\ -(l+1)\,, & \text{for} \quad j = l + \dfrac{1}{2} \end{cases} = \pm \left(j + \frac{1}{2} \right).$$

Equation (146) can now be rewritten in the form of the Schrödinger equation

$$-K_0^3 u'' + V_{[j,l]}(p)\, u = E u \tag{147}$$

with the effective potential

$$V_{[j,l]}(p) = E_p + K_0^3 \left[\frac{\varphi_p'^2}{4} + \frac{\kappa}{p^2} (\kappa + \sin\varphi_p) \right]. \tag{148}$$

We note that the well-known property of the spherical spinors

$$\boldsymbol{\sigma} \hat{\mathbf{p}}\, \Omega_{jlm}(\hat{\mathbf{p}}) = -\Omega_{jl'm}(\hat{\mathbf{p}})\,, \quad l + l' = 2j\,, \tag{149}$$

guarantees the opposite parity of the states with $j = l \pm 1/2$. Using the explicit form of effective potential (148), it is easy to find the difference between the potentials for the states with $\kappa = \pm(j + 1/2)$:

$$\Delta V = -\frac{(2j+1)\, K_0^3}{p^2} \sin\varphi_p\,, \tag{150}$$

which explicitly demonstrates the relation between the splitting in mass for the opposite-parity states and chiral symmetry, which was already discussed above in general terms. Obviously, for highly excited states with larger mean values of the relative momentum, the chiral angle decreases (see Fig. 1), as does the potential responsible for the splitting of the opposite-parity energy levels.

This type of behavior is clearly seen from the explicit solution of Eqn (147) quoted in Tables 1 and 2 and shown in Fig. 5. For clarity, we compare the obtained solutions with

Table 1. Masses of orbitally excited states and their splittings for the radial quantum number $n = 0$ resulting from the solution of exact equation (147) with potential (148) and from approximate Salpeter equation (150). All energies are given in units of the parameter K_0.

j	1/2	3/2	5/2	7/2	j	1/2	3/2	5/2	7/2
$E_{l=j-1/2}$	2.04	3.51	4.51	5.35	$E^{\text{Sapl}}_{l=j-1/2}$	2.34	3.36	4.24	5.05
$E_{l=j+1/2}$	2.66	3.69	4.57	5.36	$E^{\text{Salp}}_{l=j+1/2}$	3.36	4.24	5.05	5.79
ΔE_j	0.62	0.18	0.06	0.01	ΔE_j^{Salp}	1.02	0.88	0.81	0.74

Table 2. The same as in Table 1 but for $n = 1$.

j	1/2	3/2	5/2	7/2	j	1/2	3/2	5/2	7/2
$E_{l=j-1/2}$	3.91	5.03	5.87	6.60	$E^{\text{Sapl}}_{l=j-1/2}$	4.09	4.88	5.63	6.33
$E_{l=j+1/2}$	4.39	5.17	5.92	6.61	$E^{\text{Salp}}_{l=j+1/2}$	4.88	5.63	6.33	7.00
ΔE_j	0.48	0.14	0.05	0.01	ΔE_j^{Salp}	0.79	0.75	0.70	0.67

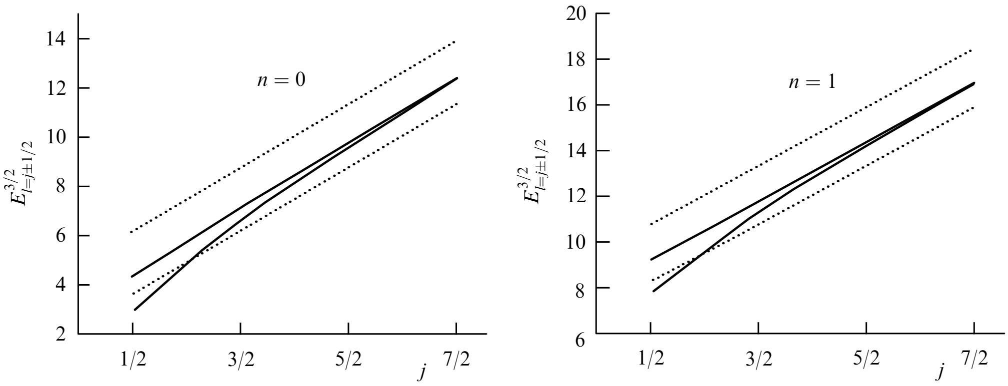

Figure 5. Regge trajectories for Eqn (147) with potential (148) (solid line) and for Salpeter equation (151) (dashed line). The respective lower and upper line correspond to $l=j-1/2$ and $l=j+1/2$.

those for the naive Salpeter equation,

$$\left[\sqrt{\mathbf{p}^2+m^2}+K_0^3\mathbf{x}^2\right]\psi(\mathbf{x})=E\psi(\mathbf{x})\,, \tag{151}$$

as derived from Eqn (147) by the substitution $E_p=\sqrt{p^2+m^2}$ and $\varphi_p\equiv\pi/2$ in potential (148),

$$V^{\mathrm{Salp}}_{[j,l]}(p)=\sqrt{p^2+m^2}+K_0^3\,\frac{\kappa(\kappa+1)}{p^2}$$
$$=\sqrt{p^2+m^2}+K_0^3\,\frac{l(l+1)}{p^2}\,. \tag{152}$$

Because the opposite-parity states correspond to the angular momenta differing by one unit, in analogy with Eqn (150), we can find that

$$\Delta V^{\mathrm{Salp}}=-\frac{2(l+1)\,K_0^3}{p^2}\,. \tag{153}$$

The semiclassical spectrum of Eqn (151) demonstrates a linear dependence of $E^{3/2}$ ($E^{(\alpha+1)/\alpha}$ with $\alpha=2$) on the angular momentum l, such that, for a given radial quantum number n, Eqn (151) produces two parallel trajectories $E^{3/2}(j)$ with $l=j\pm1/2$. For small j, similar trajectories for Eqn (147) with potential (148) have a level splitting comparable to the above-mentioned trajectories for the naive Salpeter equation, which, however, decreases fast with the growth of the angular momentum l.

This calculation explicitly demonstrates the phenomenon of effective chiral symmetry restoration in the spectrum of highly excited mesons in the GNJL model. As can be seen by just comparing potentials (150) and (153),

$$E-E'\propto\langle\sin\varphi_p\rangle\,, \tag{154}$$

where E and E' are the energies of the opposite-parity states, and averaging over the radial wave function is assumed in the right-hand side.

5.4 Pion decoupling from excited mesons

One of specific predictions for highly excited hadrons with effectively restored chiral symmetry is the decoupling of the chiral pion from them, which manifests itself through a decrease in the corresponding coupling constant with an increase in the hadron excitation number [8, 87–90]. This behavior of the coupling can be readily established with the help of the Goldberger–Treiman relation for the transitions $\mathrm{n}\to\mathrm{n}'+\pi$, where n and n$'$ are chiral partners, that is, opposite-parity hadronic states that become degenerate in mass if chiral symmetry is restored in the spectrum.[5]

We first restrict ourselves to the BCS approximation and show that the pion coupling to excited hadrons is defined by the effective mass of the dressed quark. For this, we consider the axial-vector current (for simplicity, we consider the single-flavor case and omit the chiral anomaly),

$$J^5_\mu(x)=\bar q(x)\,\gamma_\mu\gamma_5 q(x)\,, \tag{155}$$

which, due to the hypothesis of the partial conservation of the axial-vector current (PCAC), is related to the wave function of the chiral pion ϕ_π,

$$J^5_\mu(x)=f_\pi\partial_\mu\phi_\pi(x)\,. \tag{156}$$

Then, with the help of Eqn (156), it is easy to average the divergence of this current, $\partial_\mu J^5_\mu$, between the states of dressed quarks,

$$\left\langle q(p)|\partial_\mu J^5_\mu(x)|q(p')\right\rangle=f_\pi m_\pi^2\langle q(p)|\phi_\pi(x)|q(p')\rangle$$
$$\propto f_\pi g_\pi(q^2)(\bar u_p\gamma_5 u_{p'})\,,\quad q=p-p'\,, \tag{157}$$

where we have introduced the pion–quark–quark form factor $g_\pi(q^2)$.

On the other hand, if chiral symmetry is spontaneously broken and the quark wave functions obey the effective Dirac equation with the dynamically generated mass $m_{\mathrm{q}}^{\mathrm{eff}}$, then, with the help of Eqn (155), it is easy to arrive at

$$\left\langle q(p)|\partial_\mu J^5_\mu(x)|q(p')\right\rangle\propto m_{\mathrm{q}}^{\mathrm{eff}}(\bar u_p\gamma_5 u_{p'})\,. \tag{158}$$

Equating the right-hand sides of Eqns (157) and (158), we find that

$$f_\pi g_\pi=m_{\mathrm{q}}^{\mathrm{eff}}\,,\quad g_\pi\equiv g_\pi(m_\pi^2)\,, \tag{159}$$

[5] Strictly speaking, the Goldberger–Treiman relation connects the pion–nucleon constant with the nucleon axial constant; the derivation of this relation can be found in any textbook on strong interactions. Notwithstanding that, we hereafter use the name of Goldberger–Treiman relation to denote the one for the pion–hadron coupling constant $g_{\mathrm{nn}'\pi}$.

where all numerical coefficients are absorbed into the definition of the coupling constant g_π for simplicity. It follows from Eqn (11) that the effective mass of the quark is described by the quantity A_p. Then, with the help of relation (159), it is straightforward to finally find that [91]

$$f_\pi g_\pi(p) \simeq A_p \,. \tag{160}$$

Beyond the BCS level, the Goldberger–Treiman relation connects the pion coupling constant with an excited hadron exhibiting mass splitting between the two hadronic chiral partners. For definiteness, we consider the transition $\bar{\mathrm{D}}(J^P = 0^+) \to \bar{\mathrm{D}}'(J^P = 0^-)\,\pi$, where the quark content of the $\bar{\mathrm{D}}^{(\prime)}$ meson is $\bar{\mathrm{c}}\mathrm{q}$ with the light quark $\mathrm{q} = \mathrm{u}, \mathrm{d}$.

From PCAC condition (156) generalized to the isospin group SU(2), we obtain

$$\left\langle 0|J_\mu^{5a}(0)|\pi^b(\mathbf{q})\right\rangle = \mathrm{i} f_\pi q_\mu \delta_{ab} \,, \tag{161}$$

whence the transition matrix element $\left\langle n'|J_\mu^{5a}|n\right\rangle$ ($n^{(\prime)} = \bar{D}^{(\prime)}$) is easily found as

$$\left\langle n'|J_\mu^{5a}|n\right\rangle = \left\langle n'|J_\mu^{5a}|n\right\rangle_{\mathrm{nonpion}} - \frac{2Mq_\mu f_\pi g_{\mathrm{nn'}\pi}}{q^2 - M_\pi^2 + \mathrm{i}0}\, D'^{\dagger}\tau^a D \,, \tag{162}$$

where we introduce the pion coupling constant $g_{\mathrm{nn'}\pi}$ and the isospin doublets D and D'.

On the other hand, it is easy to establish the most general form of the left-hand side of Eqn (162) compatible with Lorentz invariance,

$$\left\langle n'|J_\mu^{5a}|n\right\rangle = \big[(P_\mu + P'_\mu)\, G_A(q^2) - (P_\mu - P'_\mu)\, G_S(q^2)\big]\, D'^{\dagger}\left(\frac{\tau^a}{2}\right) D \,, \tag{163}$$

where P_μ and P'_μ are the momenta of the respective initial and final D meson, and $q_\mu = P_\mu - P'_\mu$. Then, in the leading order in the heavy-quark mass, the axial-vector current conservation leads to the condition

$$2M(M - M')\, G_A - q^2 G_S = 0 \,. \tag{164}$$

From relation (162), we can see that in the limit $q^2 \to 0$, we have $G_A(0) \equiv G_A \neq 0$ if G_S is identified with the pion pole, that is,

$$\lim_{q^2 \to 0} G_S(q^2) \to \frac{4Mf_\pi g_{\mathrm{nn'}\pi}}{q^2} \,. \tag{165}$$

The resulting equation

$$\frac{1}{2}\,(M - M')\, G_A = f_\pi g_{\mathrm{nn'}\pi} \,, \tag{166}$$

is nothing more than the sought Goldberger–Treiman relation for heavy–light mesons. This relation implies that as the excitation of D grows, and therefore its degeneracy with its chiral partner D$'$ becomes more manifested, the pion decouples from this meson.

We now derive relations (160) and (166) microscopically. We consider the pion emission process by a hadron n (here, hadrons n and n$'$ are mesons; the case of baryons is studied in Section 5.5), $\mathrm{n} \to \mathrm{n}' + \pi$. The corresponding diagrams are depicted in Fig. 6, and the matrix element is given by

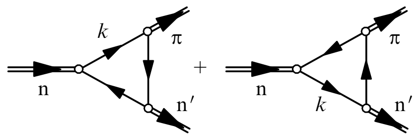

Figure 6. Transition amplitude $\mathrm{n} \to \mathrm{n}' + \pi$.

$$M(\mathrm{n} \to \mathrm{n}' + \pi) = \int \frac{\mathrm{d}^4 k}{(2\pi)^4}\, \mathrm{Sp}\big[\chi_{\mathrm{n}}(\mathbf{k}, \mathbf{P})\, S(k - P) \times \bar{\chi}_{\mathrm{n}'}(\mathbf{k} - \mathbf{P}, \mathbf{P}')\, S(k - q)\, \bar{\chi}_\pi(\mathbf{k}, \mathbf{q})\, S(k)\big] + \int \frac{\mathrm{d}^4 k}{(2\pi)^4}\, \mathrm{Sp}\big[\chi_{\mathrm{n}}(\mathbf{k}, \mathbf{P})\, S(k - P)\, \bar{\chi}_\pi(\mathbf{k}, \mathbf{q}) \times S(k - q)\, \bar{\chi}_{\mathrm{n}'}(\mathbf{k} - \mathbf{P}, \mathbf{P}')\, S(k)\big] \,, \tag{167}$$

where $q = P - P'$ and each hadronic vertex contains an amplitude χ ($\bar{\chi}$ for the outgoing meson) that satisfies Bethe–Salpeter equation (33). Thus, the pion emission vertex is given by the overlap of three vertex functions. The maximal overlap is achieved if the wave functions of all three mesons are localized in the same region in momentum. As it happens, pion wave function (44) is localized at small relative momenta between the quark and the antiquark, and it decreases fast as the momentum increases. The wave functions of the mesons n and n$'$ are localized at approximately the same momenta, which grow with the excitation number. This implies that the overlap of the vertex functions decreases with the growth of the excitation of the meson n, as does the pion coupling constant.

To describe this effect quantitatively, we write the matrix vertex $\chi(\mathbf{p}, \mathbf{P})$ in terms of the matrix wave function defined in Eqn (44),

$$\chi(\mathbf{p}, \mathbf{P}) = \int \frac{\mathrm{d}^3 k}{(2\pi)^3}\, V(\mathbf{p} - \mathbf{k})\, \gamma_0 \tilde{\phi}(\mathbf{k}, \mathbf{P})\, \gamma_0 \,. \tag{168}$$

The matrix vertex for the incoming meson is simply related to the vertex for the outgoing meson,

$$\bar{\chi}(\mathbf{p}, \mathbf{P}) = \gamma_0 \chi^\dagger(\mathbf{p}, \mathbf{P})\, \gamma_0 \,. \tag{169}$$

The explicit form of the matrix wave function $\tilde{\phi}_\pi$ for a pion at rest ($\mathbf{P}_\pi \equiv \mathbf{q} \to 0$) is given by Eqn (59), while the components $\varphi_\pi^{\pm}$ are quoted in Eqn (55). It is then easy to find for the pion emission vertex $\bar{\chi}_\pi(\mathbf{p}, \mathbf{q} = 0) \equiv \bar{\chi}_\pi(\mathbf{p})$ that

$$f_\pi \bar{\chi}_\pi(\mathbf{p}) = \sqrt{\frac{2\pi N_{\mathrm{c}}}{m_\pi}}\, \gamma_5 \int \frac{\mathrm{d}^3 k}{(2\pi)^3}\, V(\mathbf{p} - \mathbf{k})\, \sin\varphi_k = \mathrm{const} \times \gamma_5 A_p \,, \tag{170}$$

where definition (11) of the function A_p is used. If the pion form factor $g_\pi(p)$ is defined with the same constant as in Eqn (170),

$$\bar{u}_p \bar{\chi}_\pi(\mathbf{p})\, u_p = \mathrm{const} \times g_\pi(p)(\bar{u}_p \gamma_5 u_p) \,, \tag{171}$$

then we finally arrive at the Goldberger–Treiman relation in the form

$$f_\pi g_\pi(p) = A_p \,, \tag{172}$$

which coincides with formula (160), but now this relation is derived rigorously.

We emphasize an essential difference between Eqns (172) and (159), with the latter taken naively. Indeed, naively, one could conclude that the right-hand side of (159) contains a quantity that depends only on the momentum transfer in the pion emission vertex, that is, on the pion momentum $q = 0$. Then $m_{\rm q}^{\rm eff}$ has to be treated as a constant, independent of the excitation number of the hadron that emits the pion. The same would be true for the pion coupling g_π. However, the microscopic treatment expounded above demonstrates that the pion emission vertex is a function of two variables: the pion momentum and the loop momentum floating through the pion emission vertex. The latter quantity also plays the role of the momentum of the quark interacting with the pion. Therefore, even in the limit $q = 0$, the right-hand side of (172) is a decreasing function of the momentum rather than a constant. It is easy to estimate its decrease rate. Indeed, in the chiral limit, $A_p = E_p \sin\varphi_p$, while for large momenta, $E_p \approx p$ with the chiral angle behaving as $\varphi_p \propto 1/p^{4+\alpha}$, where α is the parameter of the power-law potential [see Eqn (25)]. Thus,

$$g_\pi(p) \underset{p\to\infty}{\sim} \frac{1}{p^{\alpha+3}} \,. \tag{173}$$

The result of the numerical calculation of the ratio $g_\pi(p)/g_\pi(0)$ for the harmonic oscillator potential ($\alpha = 2$), given in Fig. 7, shows that the pion coupling does decrease as the quark momentum increases.

To conclude this section, we derive Goldberger–Treiman relation (166) for the pion emission by a heavy–light meson microscopically [92].

First, we proceed from the nonrelativistic normalization (57) for pion wave functions (55) to the relativistic one, and we therefore define the wave functions

$$X_p = \frac{\sqrt{N_{\rm c}}}{f_\pi}\left(\sin\varphi_p + M_\pi \Delta_p\right), \;\; Y_p = \frac{\sqrt{N_c}}{f_\pi}\left(\sin\varphi_p - M_\pi \Delta_p\right). \tag{174}$$

We can then find that

$$\int \frac{{\rm d}^3 p}{(2\pi)^3}\left(X_p^2 - Y_p^2\right) = 2M_\pi, \tag{175}$$

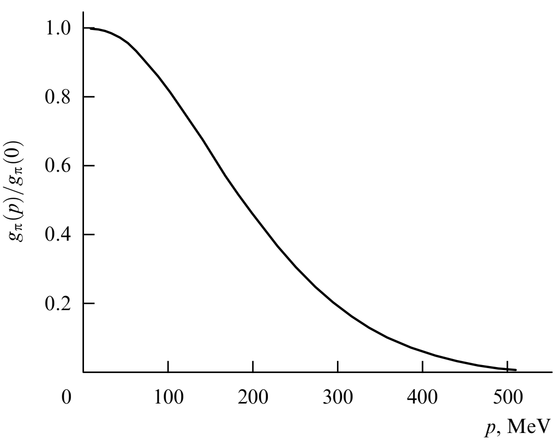

Figure 7. Dependence of the ratio $g_\pi(p)/g_\pi(0)$ on the momentum evaluated for the harmonic oscillator potential. For definiteness, the parameter K_0 is fixed as in Eqn (143).

and the pionic field with the isospin projection a in its rest frame can be written in the form

$$|\pi^a\rangle = \frac{1}{\sqrt{N_{\rm c}}}\sum_{\alpha=1}^{N_{\rm c}} \sum_{s_1, s_2 = \uparrow,\downarrow} (\sigma_2)_{s_1 s_2} \sum_{i_1, i_2 = \pm 1/2} \left(\frac{\tau^a}{2}\right)^{i_1 i_2} \int \frac{{\rm d}^3 p}{(2\pi)^3}$$
$$\times \left[b^\dagger_{\alpha s_1 i_1}(\mathbf{p})\, d^{\alpha\dagger}_{s_2 i_2}(-\mathbf{p})\, X_p + d^\alpha_{s_2 i_2}(-\mathbf{p})\, b_{\alpha s_1 i_1}(\mathbf{p})\, Y_p\right]|0\rangle \,, \tag{176}$$

where $|0\rangle$ is the BCS vacuum.

The wave functions of the pseudoscalar and scalar heavy–light mesons that obey Eqns (113) and (139) can be written in the form

$$\psi(\mathbf{p}) = \frac{\rm i}{\sqrt{2}}\,\sigma_2 \phi_p \,, \quad \psi'(\mathbf{p}) = \boldsymbol{\sigma}\hat{\mathbf{p}}\,\psi(\mathbf{p}) = \frac{\rm i}{\sqrt{2}}\,\boldsymbol{\sigma}\hat{\mathbf{p}}\,\sigma_2 \phi'_p \tag{177}$$

and normalized by the relativistic conditions

$$\begin{aligned} &{\rm Tr}\int \frac{{\rm d}^3 p}{(2\pi)^3}\,\left|\psi(\mathbf{p})\right|^2 = \int \frac{{\rm d}^3 p}{(2\pi)^3}\,\phi_p^2 = 2M\,, \\ &{\rm Tr}\int \frac{{\rm d}^3 p}{(2\pi)^3}\,\left|\psi'(\mathbf{p})\right|^2 = \int \frac{{\rm d}^3 p}{(2\pi)^3}\,\phi_p'^2 = 2M', \end{aligned} \tag{178}$$

where the trace is taken in the spin indices. Moreover, we can set $M = M'$ in the above normalization conditions.

The pion coupling constant $g_{{\rm nn}'\pi}$ is defined by the relation

$$\left\langle \bar{D}'\pi^a|V|\bar{D}\right\rangle = 2M{\rm i}g_{{\rm nn}'\pi}(D'^\dagger \tau^a D)(2\pi)^3 \delta^{(3)}(\mathbf{P}' + \mathbf{q} - \mathbf{P})\,, \tag{179}$$

where V is the interaction responsible for the pion emission. In what follows, we evaluate the matrix element in the left-hand side of (179) in the framework of the GNJL model.

In Fig. 8, we draw the four diagrams contributing to the matrix element $\langle \bar{D}'\pi|V|\bar{D}\rangle$, for which we can then write

$$\begin{aligned} &\left\langle \bar{D}'\pi^a|V|\bar{D}\right\rangle \\ &\quad = 2M\left[A^a_X + B^a_Y + C^a_X + D^a_Y\right](2\pi)^3\delta^{(3)}(\mathbf{P}' + \mathbf{q} - \mathbf{P}), \end{aligned} \tag{180}$$

where the contributions A^a_X and B^a_Y cancel each other, while the amplitudes C^a_X and D^a_Y take the form [92]

$$\begin{aligned} C^a_X &= \frac{(D'\tau^a D)}{4M\sqrt{N_{\rm c}}}\int \frac{{\rm d}^3 k}{(2\pi)^3}\,\frac{{\rm d}^3 p}{(2\pi)^3}\,\phi'_p V(\mathbf{p} - \mathbf{k}) \\ &\quad\times X_k \phi_k [S_p C_k - \hat{\mathbf{p}}\hat{\mathbf{k}}\, C_p S_k]\,, \\ D^a_Y &= \frac{(D'\tau^a D)}{4M\sqrt{N_{\rm c}}}\int \frac{{\rm d}^3 k}{(2\pi)^3}\,\frac{{\rm d}^3 p}{(2\pi)^3}\,\phi'_p V(\mathbf{p} - \mathbf{k}) \\ &\quad\times Y_p \phi_k [S_p C_k - \hat{\mathbf{p}}\hat{\mathbf{k}}\, C_p S_k]\,, \end{aligned} \tag{181}$$

where C_p and S_p are defined in (40) and their products follow from the vertices shown in the diagrams as black dots and given by various products of dressed quark bispinors (6). For instance, in the amplitude A^a_X (see Fig. 8), we have the combination

$$u^\dagger(\mathbf{p})\,u(\mathbf{k}) = C_p C_k + (\boldsymbol{\sigma}\hat{\mathbf{p}})(\boldsymbol{\sigma}\hat{\mathbf{k}})\,S_p S_k\,. \tag{182}$$

Now, taking relations (179)–(181) together and using the explicit form of pion wave functions (174), it is easy to find the

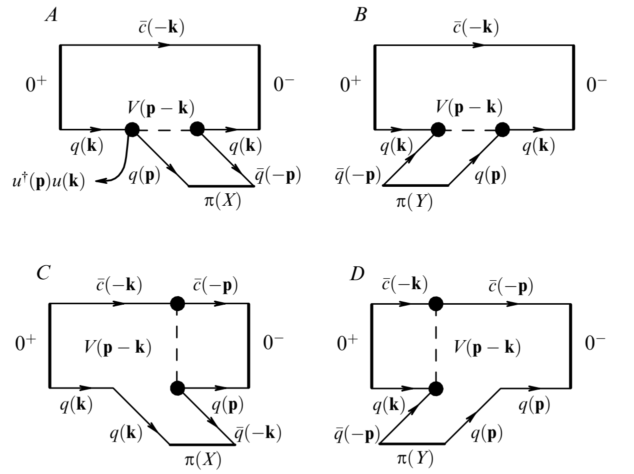

Figure 8. Diagrams contributing to the matrix element $\langle \bar{D}'\pi|V|\bar{D}\rangle$.

coupling constant $g_{\mathrm{nn}'\pi}$ in the leading order in M_π [92]:

$$f_\pi g_{\mathrm{nn}'\pi} = \frac{1}{2M}\int\frac{\mathrm{d}^3k}{(2\pi)^3}\frac{\mathrm{d}^3p}{(2\pi)^3}\,\phi'_p V(\mathbf{p}-\mathbf{k})\times$$
$$\times\,\phi_k(\sin\varphi_p+\sin\varphi_k)\big[S_pC_k-\hat{\mathbf{p}}\hat{\mathbf{k}}\,C_pS_k\big]\,. \qquad (183)$$

The non-pion contribution to the off-diagonal axial charge G_A can be evaluated with the help of the explicit expression for the temporal component of the axial-vector current, and it takes the form [92]

$$G_A = \frac{1}{2M}\int\frac{\mathrm{d}^3k}{(2\pi)^3}\,\phi'_k\phi_k\cos\varphi_k\,. \qquad (184)$$

To proceed, we multiply Eqn (113) for the wave function $\psi(\mathbf{p})$ by $\psi'(\mathbf{p})\cos\varphi_p$, take the trace in the spinor indices, and integrate both sides of the resulting equation over the momentum $\mathrm{d}^3p/(2\pi)^3$. Then we repeat the above procedures for Eqn (139) for the wave function $\psi'(\mathbf{p})$, now multiplied by $\psi(\mathbf{p})\cos\varphi_p$. Subtracting one resulting equation from the other, we arrive at the relation

$$\frac{1}{2}\,(E-E')\,G_A = \frac{1}{2M}\int\frac{\mathrm{d}^3k}{(2\pi)^3}\frac{\mathrm{d}^3p}{(2\pi)^3}\,\phi'_p V(\mathbf{p}-\mathbf{k})$$
$$\times\,\phi_k\big[\cos\varphi_p(C_pC_k+\hat{\mathbf{p}}\hat{\mathbf{k}}\,S_pS_k)$$
$$-\cos\varphi_k(\hat{\mathbf{p}}\hat{\mathbf{k}}\,C_pC_k+S_pS_k)\big]\,. \qquad (185)$$

After simple trigonometric transformations, the right-hand side of the last equation reduces to that in (183). Therefore, equating the left-hand sides of Eqns (183) and (185) and proceeding from the energies E and E' to the corresponding masses (that is, adding the mass of the heavy antiquark), we finally arrive at Goldberger–Treiman relation (166).

Two comments are in order here. On the one hand, it is easy to see that the role played by the Y (φ_π^-) component of the pion wave function in the derivation of relation (166) is as important as the role of the component X (φ_π^+). This once more emphasizes the Goldstone nature of the chiral pion, which, as a matter of principle, cannot be described in naive (constituent) quark models.

On the other hand, it follows from Eqn (184), from the properties of the chiral angle, and from normalization condition (177) that the axial charge approaches unity for excited mesons, $G_A \underset{n\to\infty}{\longrightarrow} 1$. Therefore, as stated above, the pion coupling constant decreases for highly excited mesons:

$$g_{\mathrm{nn}'\pi} = \frac{G_A\Delta M_\pm}{2f_\pi}\propto\Delta M_\pm \underset{n\to\infty}{\longrightarrow} 0\,, \qquad (186)$$

and that implies that the Goldstone boson decouples from the spectrum of excited heavy–light quarkonia.

5.5 Effective chiral symmetry restoration in the spectrum of excited baryons

In Sections 5.3 and 5.4, we studied in detail the problem of the effective restoration of chiral symmetry in the spectrum of highly excited hadrons and the related question of the chiral pion (Goldstone boson) decoupling from the spectrum of highly excited mesons. A similar situation takes place in the spectrum of excited baryons. We start from a general symmetry-based discussion.

We consider a chiral doublet B built from the effective baryonic fields B_+ and B_- of opposite parities [54],

$$B = \begin{pmatrix} B_+ \\ B_- \end{pmatrix}. \qquad (187)$$

The states B_+ and B_- are mixed by the axial transformation

$$B\to\exp\left(\mathrm{i}\,\frac{\theta_A^a\tau^a}{2}\,\sigma_1\right)B\,, \qquad (188)$$

where σ_1 is the Pauli matrix in the space of the doublet B. It is easy to establish the form of the Lagrangian invariant under the above transformation (for alternative forms of this Lagrangian, see [93, 94]):

$$\mathcal{L}_0 = \mathrm{i}\bar{B}\gamma^\mu\partial_\mu B - m_0\bar{B}B = \mathrm{i}\bar{B}_+\gamma^\mu\partial_\mu B_+ + \mathrm{i}\bar{B}_-\gamma^\mu\partial_\mu B_-$$
$$-\,m_0\bar{B}_+B_+ - m_0\bar{B}_-B_-\,. \qquad (189)$$

An important property of this Lagrangian is the presence of a nonvanishing chirally invariant mass m_0, the same for opposite-parity fields. This implies the Wigner–Weyl realization of chiral symmetry with massive fermions. Chiral doublets are inevitable in this scenario.

Therefore, in the spectrum of baryons, in addition to the 'standard' scenario when the fermion mass emerges as a result of spontaneous chiral symmetry breaking (Nambu–Goldstone realization), an alternative realization consistent with chiral doublets is possible. It is straightforward to build the Noether current that corresponds to symmetry (188) of Lagrangian (189):

$$j^a_{5\mu} = \bar{B}_+\gamma_\mu\,\frac{\tau^a}{2}\,B_- + \bar{B}_-\gamma_\mu\,\frac{\tau^a}{2}\,B_+\,. \qquad (190)$$

It does not contain diagonal terms of the form either $\bar{B}_+\gamma_\mu\gamma_5(\tau^a/2)\,B_+$ or $\bar{B}_-\gamma_\mu\gamma_5(\tau^a/2)\,B_-$. Therefore, the diagonal axial charges of the baryons B_+ and B_- that form the chiral doublet vanish, while the off-diagonal axial charges related to transitions between the opposite-parity states equal unity [54]:

$$G_A^+ = G_A^- = 0\,,\quad G_A^{+-} = G_A^{-+} = 1\,. \qquad (191)$$

We note that the axial charge of the standard Dirac fermion equals 1.

It is easy to trace the consequences of property (191). First, the diagonal pion couplings to baryons must vanish together with the diagonal axial charges of the baryons, that is, $g_{\pi B_\pm B_\pm} = G_A^\pm m_\pm / f_\pi = 0$.

Below, we derive the formulas for the off-diagonal constant $g_{\pi B_+ B_-}$. For this, we consider the matrix element of the axial-vector current between two arbitrary opposite-parity baryonic states $1/2^+$ and $1/2^-$:

$$\left\langle B_-(p_{\rm f}) | j^a_{5\mu} | B_+(p_{\rm i}) \right\rangle = \bar u(p_{\rm f}) \big(\gamma_\mu H_1(q^2) + \sigma_{\mu\nu} q^\nu H_2(q^2) + q_\mu H_3(q^2) \big) \frac{\tau^a}{2} u(p_{\rm i}) , \tag{192}$$

where $p_{\rm i}$ and $p_{\rm f}$ are the initial- and final-state momenta ($q = p_{\rm f} - p_{\rm i}$), and we introduce the form factors H_1, H_2, and H_3. For the matrix element of the divergence of the axial-vector current, we then arrive at

$$\left\langle B_-(p_{\rm f}) | \partial^\mu j^a_{5\mu} | B_+(p_{\rm i}) \right\rangle = {\rm i} \left[(m_+ - m_-)\, H_1(q^2) + q^2 H_3(q^2) \right] \bar u(p_{\rm f}) \frac{\tau^a}{2} u(p_{\rm i}) . \tag{193}$$

Inasmuch as the left-hand side of (193) vanishes in the chiral limit due to the PCAC condition, in the limit $q \to 0$, the form factors must obey the condition

$$(m_+ - m_-)\, H_1(0) + \lim_{q\to 0} q^2 H_3(q^2) = 0 , \tag{194}$$

which can be easily recognized as the Goldberger–Treiman relation

$$g_{\pi B_+ B_-} = \frac{G_A^{+-}(m_+ - m_-)}{2 f_\pi} , \quad G_A^{+-} = H_1(0) . \tag{195}$$

Indeed, PCAC requires that the contribution of the term proportional to H_1 be compensated by the term proportional to H_3, and the latter has to develop a pole at $q^2 \to 0$, which is naturally identified with the Goldstone pole. Thus, if the states $B^\pm$ belong to the same chiral doublet, they become degenerate in the mass, which ensures that $g_{\pi B_+ B_-} = 0$, and this condition, being a consequence of PCAC, is independent of the particular degeneracy mechanism for the states $B^\pm$.

Similarly to mesons, the general symmetry-based arguments given above admit a particular microscopic realization in the framework of the GNJL model. However, it is important to comment on the baryonic states in this model. Although the model is considered in the formal limit $N_{\rm c} \to \infty$, properties of the baryons can be studied qualitatively (and in many cases also quantitatively) if $N_{\rm c} = 3$ is substituted. Then the baryon can be built by acting with the three dressed-quark operators on the BCS vacuum and contracting the result with the relevant wave function,

$$\begin{aligned} \Psi_B &= \Psi_{\rm color} \otimes \Psi_{\rm flavor} \otimes \Psi_{\rm spin} \otimes \Psi_{\rm space} , \\ \Psi_{\rm color} &= \frac{1}{3!}\, \varepsilon_{\alpha\beta\gamma} q^\alpha q^\beta q^\gamma , \end{aligned} \tag{196}$$

where $\varepsilon_{\alpha\beta\gamma}$ is the antisymmetric Levi-Civita tensor. Baryons do not bring any new effects to the model and, what is more, the Dyson equations for baryons turn out to be much simpler than the similar equations for mesons. The simplification comes from the fact that the positive-energy component of the amplitude for baryons does not couple to the negative-energy component, because such transitions would imply the existence of states with open color (Fig. 9).

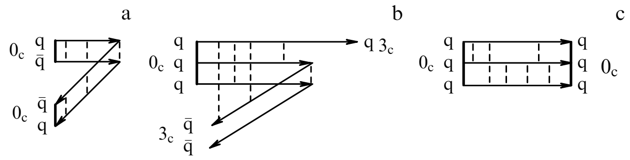

Figure 9. (a) Typical color-allowed (singlet–singlet, $0_{\rm c} \to 0_{\rm c}$) transition between the positive-energy and negative-energy amplitudes for a $q\bar q$ pair. (b) A similar transition is forbidden in a baryon because it results in a state with open color ($3_{\rm c}$). (c) A typical color-allowed diagram contributing to the Dyson equation for the baryon in the ladder approximation.

Since the color wave function of the baryon is by construction antisymmetric under permutations of the quarks, it is sufficient to study only symmetric combinations $\Psi_{\rm flavor} \otimes \Psi_{\rm spin} \otimes \Psi_{\rm space}$, such that in the general case the spatial wave function $\Psi^{\mathcal Y}_{\rm space}(\boldsymbol\rho, \boldsymbol\lambda)$ (where $\boldsymbol\rho$ and $\boldsymbol\lambda$ are the standard Jacobi coordinates) contain all possible permutations of $\mathcal Y$: antisymmetric ($\mathcal A$), symmetric ($\mathcal S$), and mixed F ($\mathcal D_F$) or D ($\mathcal D_D$). So far, all considerations have been quite general, but a particular form of some baryonic wave functions is used later in this section to calculate the axial charges of these baryons.

We consider the axial charge operator

$$Q_5^{\rm a} = \int {\rm d}^3 x\, \bar\psi_i \gamma_0 \gamma_5 \left(\frac{\tau^{\rm a}}{2} \right)^{ij} \psi_j \tag{197}$$

and evaluate it for dressed quarks using Eqns (5) and (6). The result is [95]

$$\begin{aligned} Q_5^{\rm a} = \sum_{i,j} \sum_{\alpha=1}^{N_{\rm c}} \sum_{s,\,s'=\uparrow,\downarrow} \left(\frac{\tau^{\rm a}}{2} \right)^{ij} \int \frac{{\rm d}^3 p}{(2\pi)^3} \Big[\cos\varphi_p (\boldsymbol\sigma \hat{\mathbf p})_{ss'} \\ \times \big(b^\dagger_{i\alpha s}(\mathbf p)\, b^\alpha_{js'}(-\mathbf p) + d^{\alpha\dagger}_{js}(-\mathbf p)\, d_{i\alpha s'}(\mathbf p) \big) \\ + \sin\varphi_p ({\rm i}\sigma_2)_{ss'} \big(b^\dagger_{i\alpha s}(\mathbf p)\, d^{\alpha\dagger}_{js'}(-\mathbf p) + d_{i\alpha s}(\mathbf p)\, b^\alpha_{js'}(-\mathbf p) \big) \Big] , \end{aligned} \tag{198}$$

where the two contributions in the square brackets have different physical interpretations. The first term is diagonal in the quark creation and annihilation operators (nonanomalous term) and, because it contains the operator $\boldsymbol\sigma \hat{\mathbf p}$, it is responsible for the transition from the baryonic state with a given parity to the baryonic state with the opposite parity, that is, to the chiral partner. The second term in (198) has the content of a Bogoliubov anomalous term. Since the axial current is a component of the conserved Noether current and therefore commutes with the Hamiltonian, $[Q_5^{\rm a}, H] = 0$, the state $Q_5^{\rm a}|0\rangle = |\pi^{\rm a}\rangle$ is degenerate with the vacuum and is a Goldstone boson; in other words, it is nothing more than the chiral pion. Indeed, the quantity $\sin\varphi_p({\rm i}\sigma_2)$ is the wave function of the pion in its rest frame [see Eqns (55) and (71)].

We consider the diagonal part of the axial charge operator of a baryon defined as the sum of operators (198) over all quarks in the baryon,

$$Q_5 \equiv Q_5^3 = \sum_{n=1}^{3} Q^3_{5n} . \tag{199}$$

From the above consideration, it is easy to see that the result of such an operator acting on the baryonic state can be schematically represented in the form

$$\mathcal{Q}_5|B\rangle = |B'\rangle + |B\pi\rangle\,, \tag{200}$$

where the first term in the right-hand side describes the chiral partner of the state $|B\rangle$, and the second term contains a neutral pion. The relative weight of the above two terms is defined by the chiral angle φ_p. In particular, in the case of maximal symmetry breaking, $\varphi_p = \pi/2$, and therefore only the second term survives in the right-hand side of (200). In the opposite limit of unbroken chiral symmetry, $\varphi_p = 0$, and hence only the first term survives. In this case, it is easy to arrive at the following (obvious) properties of the operator $\mathcal{Q}_5$:

$$\mathcal{Q}_5^\dagger = \mathcal{Q}_5\,, \quad \left\langle B_2|\mathcal{Q}_5^2|B_1\right\rangle \propto \left\langle B_2|B_1\right\rangle = \delta_{B_1B_2}\,. \tag{201}$$

Therefore,

$$\mathcal{Q}_5|B^\pm\rangle = G_{\mathrm{A}}^{\pm\mp}|B^\mp\rangle\,, \tag{202}$$

where $B^\pm$ stands for opposite-parity baryons and $G_{\mathrm{A}}^{\pm\mp}$ stands for axial charges. Then, for the baryon spectrum in the limit of exact chiral symmetry restoration, the following relations between various axial charges hold:

$$G_{\mathrm{A}}^{+-} = G_{\mathrm{A}}^{-+} = 1\,, \quad G_{\mathrm{A}}^{++} \equiv G_{\mathrm{A}}^{+} = 0\,, \quad G_{\mathrm{A}}^{--} \equiv G_{\mathrm{A}}^{-} = 0\,. \tag{203}$$

These relations are approached asymptotically as the excitation number of the baryon increases. Because, as was mentioned above, the axial charge operator commutes with the Hamiltonian, the states $|B^+\rangle$ and $|B^-\rangle$ should become degenerate in this limit.

5.6 Axial charges of baryons in the nonrelativistic quark model

In Section 5.5, the effective restoration of chiral symmetry in the spectrum of excited baryons was described in detail in the microscopic framework provided by the GNJL model. In particular, predictions were made for the axial charges of baryons. For comparison, we evaluate the axial charges of some baryons in a different approach. In particular, a popular alternative approach to baryons is provided by the well-known nonrelativistic SU(6) quark model, which includes the SU(3) isospin group and the SU(2) spin group and which is quite successful in describing the ground states of baryons [96, 97]. All ground-state baryons with the quantum numbers $1/2^+$ and $3/2^+$, which respectively form an octet and a decuplet of the isospin SU(3) group, enter the 56-plet of the SU(6) group. Then, for example, the magnetic moments of baryons (in fact, their ratios) are reproduced in the SU(6) model with an accuracy of about 10–15%. One of the best-known predictions of this model, the nucleon axial charge $G_A = 5/3$, coincides with the experimental value $G_A = 1.26$ quite well; the discrepancy is caused by the ignored relativistic effects, by the pionic cloud, by the effects of the SU(6) symmetry breaking because of the different quark masses, and so on.

In the large-N_{c} limit, the ground states in the spectrum of baryons indeed obey the SU(6) algebra [98, 99], which is a consequence of spontaneous chiral symmetry breaking, resulting in the emergence of large constituent quark masses. To predict the masses of the excited baryons, the SU(6) symmetry group needs to be supplied with dynamical assumptions about the structure of the radial and angular excitations of quarks in the baryons. In the simplest case of the harmonic oscillator confining potential, the energy of the quarks is fully fixed by the principal quantum number, and the masses of the excited negative-parity states of the nucleon and Δ agree well with the predictions of such an $\mathrm{SU}(6)\times\mathrm{O}(3)$ classification scheme with $N = 1$. However, for positive-parity states, this scheme meets certain difficulties, such as an overestimated splitting with negative-parity states and, for the Roper resonance, with the wrong ordering of opposite-parity levels.

In the literature, there have been successful attempts to resolve the aforementioned difficulties via a particular symmetry breaking mechanism [100]. However, a systematic mass degeneracy of opposite-parity excited baryons looks quite unnatural in the framework of this quark model, and there is no explanation for this phenomenon. In particular, in the $\mathrm{SU}(6)\times\mathrm{O}(3)$ scheme, there are no reasons whatsoever for the axial charges of the baryons to obey formula (203). Meanwhile, because the axial charges of baryons can be evaluated on the lattice (see, e.g., [97, 101–104]), it would be natural to confront the lattice results with predictions of the $\mathrm{SU}(6)\times\mathrm{O}(3)$ quark model, in which the effective restoration of chiral symmetry is not possible. Then the deviations of lattice data from the quark model predictions can be interpreted as an argument in favor of chiral symmetry restoration in the spectrum of excited baryons.

To evaluate the axial charges of baryons in the nonrelativistic quark model, we need to work out the averages over the baryon wave functions of the form

$$G_{\mathrm{fi}}^{\mathrm{A}} = \left\langle \Psi_{\mathrm{f}}(1,2,3)|\sum_{n=1}^{3} Q_n^{\mathrm{A}}|\Psi_{\mathrm{i}}(1,2,3)\right\rangle, \tag{204}$$

where Q_n^{A} is the operator of the axial charge of the nth quark, which in the leading order is given by the Gamow–Teller formula $\sigma_3\tau_3$ (where σ and τ are the respective spin and isospin operators of the Dirac fermion). This operator allows relativistic corrections (which, however, are not considered below) of the form

$$\frac{1}{2M}\,\boldsymbol{\sigma}\,(\mathbf{p}_{\mathrm{i}}+\mathbf{p}_{\mathrm{f}})\,\tau^a\exp\left(\mathrm{i}\mathbf{qr}\right), \tag{205}$$

where $\mathbf{q} = \mathbf{p}_{\mathrm{f}} - \mathbf{p}_{\mathrm{i}}$. In addition, the operator of the axial charge of a nonrelativistic quark in the leading order also contains a dependence on the spatial coordinate in the form of the exponential $\exp(\mathrm{i}\mathbf{qr})$. However, evaluation of both the diagonal and off-diagonal axial charges amounts to taking the limit $\mathbf{q}\to 0$ [105]. In the leading order, the axial charge operator is then independent of the coordinate, and therefore matrix element (204) is nonzero only if the spatial wave functions of the initial and the final baryons coincide. This prediction of the $\mathrm{SU}(6)\times\mathrm{O}(3)$ scheme appears to be at odds with the predictions of chiral symmetry restoration in the spectrum and, in particular, with its microscopic realization in the GNJL model framework [see Eqn (203)].

Evaluation of diagonal matrix elements (204) requires knowing the wave functions of baryons in the $\mathrm{SU}(6)\times\mathrm{O}(3)$ scheme, which are well known in the literature and are quoted in Table 3. Each wave function is characterized by several quantum numbers. First, there is the multiplet of the spin–

Table 3. Wave functions of some nucleons in the mass region below 2 GeV in the SU(6) scheme (see, e.g., [100]).

$N(\lambda\mu)\ L[f]_X[f]_{\rm FS}[f]_{\rm F}[f]_{\rm S}$	J^P, nucleon
$0(00)\ 0[3]_X[3]_{\rm FS}[21]_{\rm F}[21]_{\rm S}$	$\frac{1}{2}^+$, N
$2(20)\ 0[3]_X[3]_{\rm FS}[21]_{\rm F}[21]_{\rm S}$	$\frac{1}{2}^+$, $N(1440)$
$1(10)\ 1[21]_X[21]_{\rm FS}[21]_{\rm F}[21]_{\rm S}$	$\frac{1}{2}^-$, $N(1535)$ $\frac{3}{2}^-$, $N(1520)$
$1(10)\ 1[21]_X[21]_{\rm FS}[21]_{\rm F}[3]_{\rm S}$	$\frac{1}{2}^-$, $N(1650)$ $\frac{3}{2}^-$, $N(1700)$ $\frac{5}{2}^-$, $N(1675)$
$2(20)\ 2[3]_X[3]_{\rm FS}[21]_{\rm F}[21]_{\rm S}$	$\frac{3}{2}^+$, $N(1720)$ $\frac{5}{2}^+$, $N(1680)$
$2(20)\ 0[21]_X[21]_{\rm FS}[21]_{\rm F}[21]_{\rm S}$	$\frac{1}{2}^+$, $N(1710)$

Table 4. Diagonal axial charges of baryons evaluated in the framework of the SU(6) quark model.

Baryon	$N(1440)$	$N(1710)$	$N(1535)$	$N(1650)$
J^P	$1/2^+$	$1/2^+$	$1/2^-$	$1/2^-$
G_A	$5/3$	$1/3$	$-1/9$	$5/9$

flavor group SU(6) to which the given state belongs and which is encoded in the Young symbol $[f]_{\rm FS}$. In each such multiplet, the baryon wave function has a particular symmetry in the flavor space (the symbol $[f]_{\rm F}$ with $f = 3, 21, 111$) and a particular spin symmetry (the symbol $[f]_{\rm S}$ with $f = 3, 21$ for $S = 3/2$ and $S = 1/2$, respectively). Finally, the spatial part of the wave function is fixed by the angular momentum L and by the permutation symmetry $[f]_{\rm X}$, which is fixed by the Pauli principle as $[f]_X = [f]_{\rm FS}$. For a particular basis used, additional quantum numbers can arise, like the principal quantum number N in the harmonic oscillator basis or the spatial symmetry of the angular wave function $(\lambda\mu)$.

The diagonal axial charges of some baryons evaluated with the help of the wave functions quoted in Table 3 are given in Table 4 (details of the calculations can be found in [105]). The charges found allow us to compare the predictions of the SU(6) model with the predictions of the chiral restoration model. In particular, the states $N(1440)$ and $N(1535)$ form a chiral doublet, and therefore, according to the model of chiral restoration, their axial charges should be small. From Table 4, we can see that the SU(6) model also predicts a small axial charge for $N(1535)$; however, for the state $N(1440)$ the prediction of this model is rather large, exceeding unity. A similar situation occurs for another pair of chiral partners, $N(1710)$ and $N(1650)$: the SU(6) model predicts rather large values for both axial charges. Other examples of model calculations of the axial charges of excited baryons can be found in [106–110].

6. Conclusions

In this review, we discussed some aspects of the phenomenon of chiral symmetry breaking and the properties of hadrons in the framework of the GNJL model. An important feature of this model is its microscopic approach to chiral symmetry breaking in a vacuum and the presence of confinement, which allows using the model to address a wide class of problems related not only to low-lying states in the spectrum of hadrons but also to various properties of excited hadrons. In particular, the phenomenon of the effective restoration of chiral symmetry in the spectrum of excited mesons and baryons is described microscopically.

The main problems discussed in this review are as follows.

- An explicit microscopic description of the phenomenon of chiral symmetry breaking in a vacuum is given in terms of the dressed quark fields and the wave function of a chirally broken vacuum, which has the form of a coherent-like state formed by condensed ${}^3P_0$ quark–antiquark pairs.
- The bosonic Bogoliubov transformation is generalized to the case of compound meson operators, and the equivalence of the method to the approach based on the Bethe–Salpeter equation for meson amplitudes is proved.
- The interrelation between the Lorentz nature of confinement and spontaneous chiral symmetry breaking is addressed. The connection of spontaneous chiral symmetry breaking with the dynamically generated scalar interquark potential in quarkonium is traced at the microscopic level.
- The existence of two different dynamical regimes in the mass-gap equation is established from the most general arguments, and only one of them is shown to be realized in the chiral limit. For that regime, the chiral angle is shown to collapse in the classical limit, that is, the quantum nature of spontaneous chiral symmetry breaking in a vacuum is demonstrated directly.
- A detailed microscopic description of the phenomenon of effective chiral symmetry restoration in the spectrum of excited hadrons is presented in the framework of the GNJL model. In particular, both qualitative and quantitative analyses of the mass-gap equation for the model with an arbitrary power-law confining potential are presented and the existence of chirally nonsymmetric solutions is demonstrated for all such power-law potentials.
- The connection is traced between the interquark potential in quarkonium responsible for splitting between opposite-parity states and the chiral angle, which describes the effect of spontaneous chiral symmetry breaking. This potential is demonstrated to decrease fast with an increase in the excitation number of the meson.
- A microscopic derivation of the Goldberger–Treiman relation for the pion coupling constant with a heavy–light quarkonium is presented, and the pion is explicitly shown to decouple from the excited hadrons that form approximate chiral multiplets.
- A microscopic derivation of the behavior of the diagonal and off-diagonal axial charges of baryons that form approximate chiral multiplets is presented, and the results are contrasted with predictions of the $\mathrm{SU}(6)\times\mathrm{O}(3)$ quark model.

In conclusion, we mention a few questions and problems of the phenomenology of strong interactions that can be addressed using the GNJL model. First of all, it has to be pointed out that highly excited mesons made of light quarks demonstrate a higher level of degeneracy of the spectrum than just the restored chiral symmetry. In particular, the slopes of the Regge trajectories in the total spin J and in the radial quantum number n coincide with a high accuracy (see, e.g., recent paper [111]), which agrees well with the idea of the existence of the principal quantum number $n + J$ [55]. Furthermore, it was conjectured in a series of recent papers that highly excited hadrons form multiplets of the SU(4) group, which includes chiral symmetry as a subgroup [12, 112]. This hypothesis finds support on the lattice if a cute trick is employed [113, 114]: it was suggested that the properties of hadrons be investigated using field configurations after the artificial removal of the near-zero modes of the Dirac operator. Because the chiral condensate in a QCD vacuum is defined by the density of such near-zero modes [115], their removal should result in chiral symmetry restoration, and therefore all results obtained with the help of such special lattice configurations should demonstrate all implications of the restored chiral symmetry. Indeed, the result demonstrates the emergence of a rather high degeneracy in the spectrum, which is consistent with the SU(4) group [113, 114]. Building a dynamical model of a QCD string that has the above property is an important problem of theoretical high-energy physics, which can be addressed, in particular, using the experience gained from microscopic calculations in the framework of the generalized Nambu–Jona-Lasinio model.

Acknowledgments
Yu K's and A N's work was performed at the Institute of Nuclear Physics and Engineering supported by the MEPhI Academic Excellence Project (contract 02.a03.21.0005, 27.08.2013). They also acknowledge support from the Russian Foundation for Basic Research (grant 17-02-00485).

References

1. Eichten E et al. *Phys. Rev. D* **17** 3090 (1978)
2. Godfrey S, Isgur N *Phys. Rev. D* **32** 189 (1985)
3. Nambu Y, Jona-Lasinio G *Phys. Rev.* **124** 246 (1961)
4. Glozman L Ya *Phys. Lett. B* **475** 329 (2000)
5. Cohen T D, Glozman L Ya *Phys. Rev. D* **65** 016006 (2001)
6. Cohen T D, Glozman L Ya *Int. J. Mod. Phys. A* **17** 1327 (2002)
7. Glozman L Ya *Phys. Lett. B* **539** 257 (2002)
8. Glozman L Ya *Phys. Lett. B* **587** 69 (2004)
9. Glozman L Ya *Phys. Lett. B* **541** 115 (2002)
10. Denissenya M, Glozman L Ya, Lang C B *Phys. Rev. D* **89** 077502 (2014)
11. Banks T, Casher A *Nucl. Phys. B* **169** 103 (1980)
12. Glozman L Ya *Eur. Phys. J. A* **51** 27 (2015)
13. Simonov Yu A *Int. J. Mod. Phys. A* **31** 1650104 (2016)
14. Di Giacomo A et al. *Phys. Rep.* **372** 319 (2002)
15. 't Hooft G *Nucl. Phys. B* **75** 461 (1974)
16. Bars I, Green M B *Phys. Rev. D* **17** 537 (1978)
17. Donoghue J F, Golowich E, Holstein B R *Dynamics of the Standard Model* (Cambridge Monographs on Particle Physics, Nuclear Physics, and Cosmology, Vol. 2) (Cambridge: Cambridge Univ. Press, 1992)
18. Witten E *Nucl. Phys. B* **145** 110 (1978)
19. Coleman S R *Commun. Math. Phys.* **31** 259 (1973)
20. Kalashnikova Yu S, Nefed'ev A V *Phys. Usp.* **45** 347 (2002); *Usp. Fiz. Nauk* **172** 377 (2002)
21. Amer A et al. *Phys. Rev. Lett.* **50** 87 (1983)
22. Le Yaouanc A et al. *Phys. Lett. B* **134** 249 (1984)
23. Le Yaouanc A et al. *Phys. Rev. D* **29** 1233 (1984)
24. Le Yaouanc A et al. *Phys. Rev. D* **31** 137 (1985)
25. Bicudo P J de A, Ribeiro J E F T *Phys. Rev. D* **42** 1611 (1990)
26. Bicudo P J de A, Ribeiro J E F T *Phys. Rev. D* **42** 1625 (1990)
27. Bicudo P J de A, Ribeiro J E F T *Phys. Rev. D* **42** 1635 (1990)
28. Bicudo P J de A *Phys. Rev. Lett.* **72** 1600 (1994)
29. Bicudo P J de A *Phys. Rev. C* **60** 035209 (1999)
30. Bicudo P J A, Ribeiro J E F T, Nefediev A V *Phys. Rev. D* **65** 085026 (2002)
31. Nefediev A V, Ribeiro J E F T *Phys. Rev. D* **67** 034028 (2003)
32. Bicudo P J A, Nefediev A V *Phys. Rev. D* **68** 065021 (2003)
33. Nefediev A V, Ribeiro J E F T *Phys. Rev. D* **70** 094020 (2004)
34. Nefediev A V, Ribeiro J E F T *JETP Lett.* **90** 417 (2009); *Pis'ma Zh. Eksp. Teor. Fiz.* **90** 461 (2009)
35. Antonov D V, Nefediev A V, Ribeiro J E F T *JETP Lett.* **92** 721 (2010); *Pis'ma Zh. Eksp. Teor. Fiz.* **92** 803 (2010)
36. Bijnens J, Bruno C, de Rafael E *Nucl. Phys. B* **390** 501 (1993)
37. Arbuzov B A, Volkov M K, Zaitsev I V *Int. J. Mod. Phys. A* **21** 5721 (2006)
38. Volkov M K, Radzhabov A E *Phys. Usp.* **49** 551 (2006); *Usp. Fiz. Nauk* **176** 569 (2006)
39. Kalinovsky Yu L, Toneev V D, Friesen A V *Phys. Usp.* **59** 367 (2016); *Usp. Fiz. Nauk* **186** 387 (2016)
40. Adler S L, Davis A C *Nucl. Phys. B* **244** 469 (1984)
41. Kalinovsky Yu L, Kaschluhn L, Pervushin V N *Phys. Lett. B* **231** 288 (1989)
42. Bicudo P, Ribeiro J, Rodrigues J *Phys. Rev. C* **52** 2144 (1995)
43. Horvat R, Kekez D, Palle D, Klabucar D *Z. Phys. C* **68** 303 (1995)
44. Llanes-Estrada F J, Cotanch S R *Phys. Rev. Lett.* **84** 1102 (2000)
45. Gell-Mann M, Oakes R J, Renner B *Phys. Rev.* **175** 2195 (1968)
46. Goldberger M L, Treiman S B *Phys. Rev.* **111** 354 (1958)
47. Bicudo P *Phys. Rev. C* **67** 035201 (2003)
48. Adler S L *Phys. Rev.* **137** B1022 (1965)
49. Weinberg S *Phys. Rev. Lett.* **17** 616 (1966)
50. Bicudo P et al. *Phys. Rev. D* **65** 076008 (2002)
51. Gogokhia V, Kluge Gy *Phys. Rev. D* **66** 056013 (2002)
52. Bicudo P J A, Nefediev A V *Phys. Lett. B* **573** 131 (2003)
53. Kalashnikova Yu S, Nefediev A V, Volodin A V *Phys. Atom. Nucl.* **63** 1623 (2000); *Yad. Fiz.* **63** 1710 (2000)
54. Glozman L Ya *Phys. Rep.* **444** 1 (2007)
55. Glozman L Ya, Nefediev A V *Phys. Rev. D* **76** 096004 (2007)
56. Peláez J R, Ríos G *Phys. Rev. Lett.* **97** 242002 (2006)
57. Eichten E, Feinberg F *Phys. Rev. D* **23** 2724 (1981)
58. Gromes D *Z. Phys. C* **26** 401 (1984)
59. Brambilla N, Vairo A *Phys. Lett. B* **407** 167 (1997)
60. Simonov Yu A *Phys. Atom. Nucl.* **60** 2069 (1997); *Yad. Fiz.* **60** 2252 (1997)
61. Kalashnikova Yu S, Nefediev A V *Phys. Lett. B* **414** 149 (1997)
62. Simonov Yu A *Phys. Rev. D* **65** 094018 (2002)
63. Simonov Yu A, Tjon J A *Phys. Rev. D* **62** 014501 (2000)
64. Koma Y, Koma M *Nucl. Phys. B* **769** 79 (2007)
65. Biernat E P et al. *Phys. Rev. D* **89** 016005 (2014)
66. Balitsky I I *Nucl. Phys. B* **254** 166 (1985)
67. Bali G S *Phys. Rev. D* **62** 114503 (2000)
68. Shevchenko V, Simonov Yu *Phys. Rev. Lett.* **85** 1811 (2000)
69. Shevchenko V I, Simonov Yu A *Int. J. Mod. Phys. A* **18** 127 (2003)
70. Nefediev A V, Simonov Yu A *Phys. Rev. D* **76** 074014 (2007)
71. Nefediev A V *JETP Lett.* **78** 349 (2003); *Pis'ma Zh. Eksp. Teor. Fiz.* **78** 801 (2003)
72. Badalian A M, Nefediev A V, Simonov Yu A *JETP Lett.* **88** 558 (2008); *Pis'ma Zh. Eksp. Teor. Fiz.* **88** 648 (2008)
73. Badalian A M, Nefediev A V, Simonov Yu A *Phys. Rev. D* **78** 114020 (2008)
74. Bicudo P et al. *Phys. Lett. B* **442** 349 (1998)
75. Kalashnikova Yu S, Nefediev A V, Ribeiro J E F T *Phys. Rev. D* **72** 034020 (2005)
76. Allen T J, Olsson M G *Phys. Rev. D* **68** 054022 (2003)
77. Allen T J et al. *Phys. Rev. D* **70** 054012 (2004)
78. Nowak M A, Rho M, Zahed I *Acta Phys. Polon. B* **35** 2377 (2004)
79. Beane S R *Phys. Rev. D* **64** 116010 (2001)
80. Golterman M, Peris S *Phys. Rev. D* **67** 096001 (2003)
81. Afonin S S et al. *JHEP* **2004** 039 (2004)
82. Swanson E S *Phys. Lett. B* **582** 167 (2004)
83. DeGrand T *Phys. Rev. D* **69** 074024 (2004)
84. Shifman M, Vainshtein A *Phys. Rev. D* **77** 034002 (2008)
85. Glozman L Ya *Int. J. Mod. Phys. A* **21** 475 (2006)
86. Wagenbrunn R F, Glozman L Ya *Phys. Rev. D* **75** 036007 (2007)
87. Jaffe R L, Pirjol D, Scardicchio A *Phys. Rev. D* **74** 057901 (2006)
88. Jaffe R L, Pirjol D, Scardicchio A *Phys. Rev. Lett.* **96** 121601 (2006)
89. Jaffe R L, Pirjol D, Scardicchio A *Phys. Rep.* **435** 157 (2006)
90. Cohen T D, Glozman L Ya *Mod. Phys. Lett. A* **21** 1939 (2006)
91. Glozman L Ya, Nefediev A V *Phys. Rev. D* **73** 074018 (2006)
92. Nefediev A V, Ribeiro J E F T, Szczepaniak A P *Phys. Rev. D* **75** 036001 (2007)
93. DeTar C E, Kunihiro T *Phys. Rev. D* **39** 2805 (1989)
94. Jido D, Oka M, Hosaka A *Prog. Theor. Phys.* **106** 873 (2001)
95. Nefediev A V, Ribeiro J E F T, Szczepaniak A P *JETP Lett.* **87** 271 (2008); *Pis'ma Zh. Eksp. Teor. Fiz.* **87** 321 (2008)
96. Gürsey F, Radicati L A *Phys. Rev. Lett.* **13** 173 (1964)
97. Kokkedee J J J, Van Hove L *Nuovo Cimento* **42** 711 (1966)
98. Gervais J-L, Sakita B *Phys. Rev. Lett.* **52** 87 (1984)
99. Dashen R F, Manohar A V *Phys. Lett. B* **315** 425 (1993)
100. Glozman L Ya, Riska D O *Phys. Rep.* **268** 263 (1996)
101. Takahashi T T, Kunihiro T *Chin. Phys. C* **33** 1233 (2009)

102. Takahashi T T, Kunihiro T *Nucl. Phys. B Proc. Suppl.* **186** 113 (2009)
103. Erkol G, Oka M, Takahashi T T *Phys. Lett. B* **686** 36 (2010)
104. Maurer T et al., arXiv:1202.2834
105. Glozman L Ya, Nefediev A V *Nucl. Phys. A* **807** 38 (2008)
106. Choi K-S, Plessas W, Wagenbrunn R F *Phys. Rev. D* **82** 014007 (2010)
107. An C S, Riska D O *Eur. Phys. J. A* **37** 263 (2008)
108. An C S *Chin. Phys. C* **33** 1393 (2009)
109. Gallas S, Giacosa F, Rischke D H *Phys. Rev. D* **82** 014004 (2010)
110. Yuan S G, An C S, He J *Commun. Theor. Phys.* **54** 697 (2010)
111. Pang C-Q et al. *Phys. Rev. D* **92** 014012 (2015)
112. Glozman L Ya, Pak M *Phys. Rev. D* **92** 016001 (2015)
113. Glozman L Ya, Lang C B, Schröck M *Phys. Rev. D* **86** 014507 (2012)
114. Denissenya M, Glozman L Ya, Pak M *Phys. Rev. D* **91** 114512 (2015)
115. Casher A *Phys. Lett. B* **83** 395 (1979)